Journal of Medicinal Chemistry

Article

pubs.acs.org/jmc

3-Alkoxy-pyrrolo[1,2-*b*]pyrazolines as Selective Androgen Receptor Modulators with Ideal Physicochemical Properties for Transdermal Administration

Thomas Ullrich,*[,†] Sanjita Sasmal,[‡] Venkatesham Boorgu,[‡] Srinivasu Pasagadi,[‡] Srisailam Cheera,[‡] Sujatha Rajagopalan,[§] Archana Bhumireddy,[§] Dhanya Shashikumar,[‡] Shekar Chelur,[§] Charamanna Belliappa,[§] Chetan Pandit,[§] Narasimharao Krishnamurthy,[§] Subhendu Mukherjee,[§] Anuradha Ramanathan,[§] Chakshusmathi Ghadiyaram,[§] Murali Ramachandra,[§] Paulo G. Santos,[∥] Bharat Lagu,[⊥,¶] Mark G. Bock,[⊥] Mark H. Perrone,[⊥] Sven Weiler,[†] and Hansjoerg Keller*[,#]

[†]Global Discovery Chemistry and [#]Musculoskeletal Diseases, Novartis Institutes for BioMedical Research, CH-4002 Basel, Switzerland

[‡]Aurigene Discovery Technologies Ltd, Bollaram Road, Miyapur, Hyderabad 500 049, India

[§]Aurigene Discovery Technologies Ltd, 39-40, KIADB Industrial Area, Electronic City Phase II, Hosur Road, Bangalore 560 100, India

[∥]Technical Research and Development, Novartis Pharma AG, CH-4002 Basel, Switzerland

[⊥]Global Discovery Chemistry, Novartis Institutes for BioMedical Research, Cambridge Massachusetts 02139, United States

ABSTRACT: We describe the synthesis and characterization of 3-alkoxy-pyrrolo[1,2-*b*]pyrazolines as novel selective androgen receptor (AR) modulators that possess excellent physicochemical properties for transdermal administration. Compound **26** bound to human AR with an IC_{50} of 0.7 nM with great selectivity over other nuclear hormone receptors and potently activated AR in a C2C12 muscle cell reporter gene assay with an EC_{50} of 0.5 nM. It showed high aqueous solubility of 1.3 g/L at pH 7.4, and an in silico model as well as a customized parallel artificial membrane permeability assay indicated good skin permeation. Indeed, when measuring skin permeation through excised human skin, an excellent flux of 2 $\mu g/(cm^2 \cdot h)$ was determined without any permeation enhancers. In a 2 week Hershberger model using castrated rats, the compound showed dose-dependent effects fully restoring skeletal muscle weight at 0.3 mg/kg/day after subcutaneous administration with high selectivity over prostate stimulation.

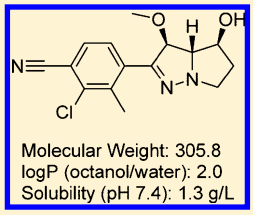

INTRODUCTION

Androgens are essential for development, maturation, and functional maintenance of the male reproductive system.[1,2] In addition, they establish secondary sex characteristics such as facial hair growth and vocal cord enlargement. Furthermore, they exert powerful anabolic actions on bone and skeletal muscle, and they decrease fat mass.[3−5] The two main endogenous androgens in men are testosterone (T) and its more potent metabolite 5α-dihydrotestosterone (DHT) generated by 5α-reductase. Most of their biological effects are mediated by binding to a single androgen receptor (AR) belonging to the nuclear receptor family of transcription factors. During male aging, T levels decrease about 1% per year, which is associated with a gradual loss of muscle mass and function, as well as the development of frailty.[6−9] Moreover, falling T levels often lead to late-onset hypogonadism (LOH) in elderly men that is characterized by low serum T levels, fatigue, and decreased libido.[10] Current therapies for LOH and other forms of male hypogonadism include different T hormone treatments.[11] However, the potential risks of T replacement such as prostate and cardiovascular safety are currently being debated.[12] Such concerns as well as potential virilizing effects in women have precluded the use of high doses of androgens as anabolics in muscle wasting diseases such as cancer cachexia and sarcopenia. To avoid this, selective androgen receptor modulators (SARMs) have been developed that selectively stimulate anabolic actions of AR in muscle and bone without inducing androgenic action in tissues such as prostate and skin.[13,14]

Several steroid-derived and nonsteroidal SARMs, all oral formulations, have entered clinical evaluation (Figure 1).[15−18] **1** (enobosarm), **2** (MK-0773) and LGD-4033 (structure not disclosed) increased lean body mass in volunteers, and **1** improved physical function in healthy elderly men and women and in cancer patients with muscle wasting.[15,16] However, the clinical potential of oral SARMs appears to be limited by the occurrence of adverse events at highly efficacious doses, for example, induction of alanine aminotransferase (ALT)[15,18] and reduction of high-density lipoprotein (HDL) in plasma.[15,17] It is therefore apparent that successful prevention of androgenic tissue stimulation by a SARM does not eliminate other putatively on-target adverse effects. Induction of signals generally associated with hepatotoxicity and unfavorable

Received: June 13, 2014
Published: August 14, 2014

 © 2014 American Chemical Society

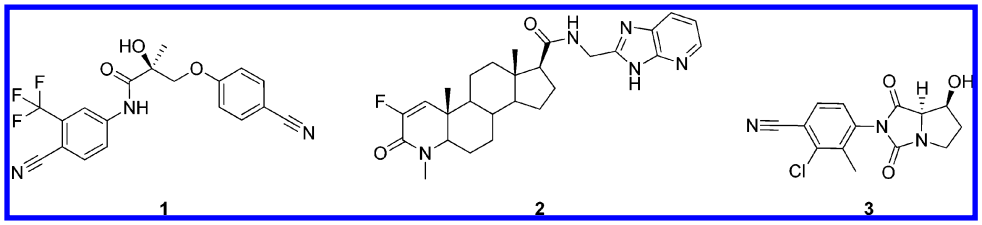

Figure 1. Exemplary steroidal and nonsteroidal SARMs that have been evaluated in clinical trials.

changes of plasma lipoproteins are well-known adverse events of oral androgen therapies.[19−21] Current T replacement therapies often use parenteral treatments such as the most frequently applied transdermal patch and gel delivery systems, which generally do not show adverse lipid changes and hepatic side effects.[20,22] With the objective to minimize high drug exposure in the liver and to provide constant drug levels to the body, we decided to fully exploit the potential of SARMs to be administered by transcutaneous routes of administration.

The ideal characteristics for passive diffusion of a compound through skin are not necessarily the same as those promoting gastrointestinal absorption. In general, the drugs currently administered across the skin fall within more stringent limits than predicted by the Rule of Five, which is commonly used to guide optimization for oral absorption.[23] Good guidelines have, however, emerged in recent years based on the wealth of drugs that have been considered−with or without success−for transdermal delivery. Ideal molecules should be small (molecular weight MW ≤400 Da), have a low melting point, high aqueous solubility, but at the same time display a balanced lipophilicity profile (partition coefficient log $P_{octanol/water}$ ∼2). Furthermore, the number of hydrogen bond donors/acceptors as well as ionizable groups which impact permeation through the cutaneous lipids at the pH of skin (it is estimated that the natural skin surface pH is on average 4.7)[24] need to be kept at a minimum. Finally, as the permeation-limited flux through skin will only allow a certain drug load to reach the systemic circulation over time, the optimal transdermal drug also has to be highly potent and efficacious in vivo to warrant low doses triggering the desired pharmacodynamic effect. Most of the drugs currently available in patch formulation share a very low required daily dose (<2 mg).[25]

Taking into consideration the physicochemical property and in vivo efficacy requirements for transdermal candidates as mentioned above, we reviewed well-described clinical and preclinical SARMs. **3** (BMS-564929, Figure 1) caught our particular attention because of its small size (MW = 305) and high potency in vitro and in vivo.[26] However, the low calculated log *P* (Clog *P* = 0.11) and low reported aqueous solubility (0.019 mg/mL)[27] of **3** would predict only limited transcutaneous permeation for the molecule. Many hydantoin-based drugs suffer from low aqueous solubility, especially when the hydantoin is attached to aromatic rings.[28] Li et al. argued that removal of one of the carbonyl groups from the hydantoin core would eliminate intermolecular hydrogen bonding between two individual molecules in the crystal lattice.[27] Further elaborating on this concept, we conceived a scaffold which would retain many of the advantages of **3** (low MW, high potency) and provide additional benefits with respect to exploring novel chemical space while not being susceptible to lactam or imide ring opening giving rise to potentially mutagenic aniline fragments. Pyrazolines were thought to be appropriate hydantoin replacements, as they can contribute to polar interactions by virtue of their nitrogen atoms without being charged at physiological pH. The privileged substitution pattern on the phenyl ring described by Li et al. remained unchanged in the course of this study, based on its beneficial impact on biological activity.[27] In this paper, we describe the synthesis and biological evaluation of 3-alkoxy-pyrrolo[1,2-*b*]pyrazolines, a novel bicyclic SARM scaffold devoid of the hydantoin substructure and with physicochemical properties suited for transdermal administration (Figure 2).

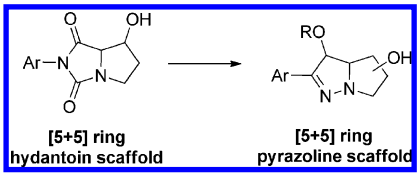

Figure 2. Restructuring the hydantoin scaffold.

■ CHEMISTRY

The first prototype was synthesized from *trans*-3-hydroxy-L-proline methyl ester (**4**) (Scheme 1). *N*-nitrosylation to **5**, followed by protection of the alcohol and chemoselective ester reduction with Superhydride, led to *N*-nitroso-prolinol **7**, which then underwent zinc-mediated reduction to hydrazine intermediate **8**.

Scheme 1. Synthesis of Hydrazine Intermediate 8 (2*R*,3*S*)[a]

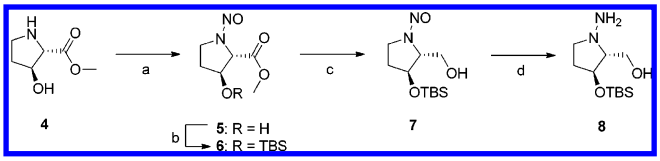

[a]Reagents and conditions: (a) $NaNO_2$, acetic acid, H_2O, 0 °C, 4 h, 68%; (b) TBS-chloride, imidazole, 25 °C, 4 h, 93%; (c) $LiEt_3BH$, THF, −78 °C, 5 h, 58%; (d) Zinc, NH_4Cl, methanol, H_2O, 50 °C, 90 min, 83%.

In a similar fashion, hydrazine intermediate **13** (2*S*,4*R*) was synthesized from L-hydroxyproline methyl ester (**9**) (Scheme 2).

Intermediate **8** was treated with 2-chloro-4-formyl-3-methylbenzonitrile (**14**)[27,29] to give hydrazone **15**, which was then subjected to Swern oxidation of the alcohol to furnish aldehyde **16**. Lewis-acid-catalyzed stereospecific cyclization[30] to intermediate **17** was then accomplished in good yield (Scheme 3).

Intermediate **13** was treated in an analogous manner to give annulated pyrazoline **20** (Scheme 4).

Deprotection of **17** yielded diol **21**, and analogues were synthesized by 3-*O*-alkylation of **17**, followed by cleavage of the silyl protective group (Scheme 5). The absolute configuration of methyl derivative **26** was unequivocally proven by

Scheme 2. Synthesis of hydrazine intermediate 13 (2*S*,4*R*)[a]

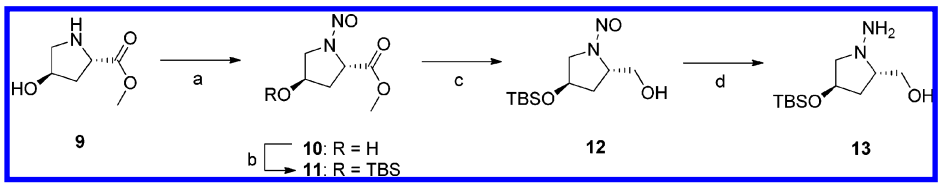

[a]Reagents and conditions: (a) $NaNO_2$, acetic acid, H_2O, 0 °C, 4 h, quant.; (b) TBS-chloride, imidazole, 25 °C, 4h, 87%; (c) $LiEt_3BH$, THF, −78 °C, 5 h, 67%; (d) Zinc, NH_4Cl, methanol, H_2O, 50 °C, 90 min, 97%.

Scheme 3. Synthesis of Pyrazoline Intermediate 17[a]

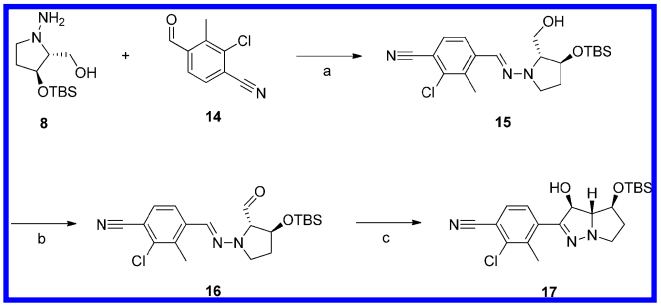

[a]Reagents and conditions: (a) acetic acid, 25 °C, 3 h, 66%; (b) oxalyl chloride, DMSO, DCM, −78 °C, 30 min, 94%; (c) $BF_3{\cdot}OEt_2$, DCM, 0 °C, 3 h, 60%.

Scheme 4. Synthesis of Pyrazoline Intermediate 20[a]

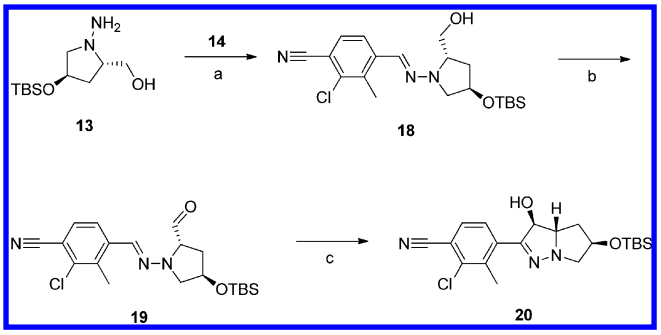

[a]Reagents and conditions: (a) acetic acid, 25 °C, 3 h, 44%; (b) oxalyl chloride, DMSO, DCM, −78 °C, 30 min, quant.; (c) $BF_3{\cdot}OEt_2$, DCM, 0 °C, 3 h, 50%.

Scheme 5. Alkylation and Deprotection of the Pyrazoline Intermediate 17[a]

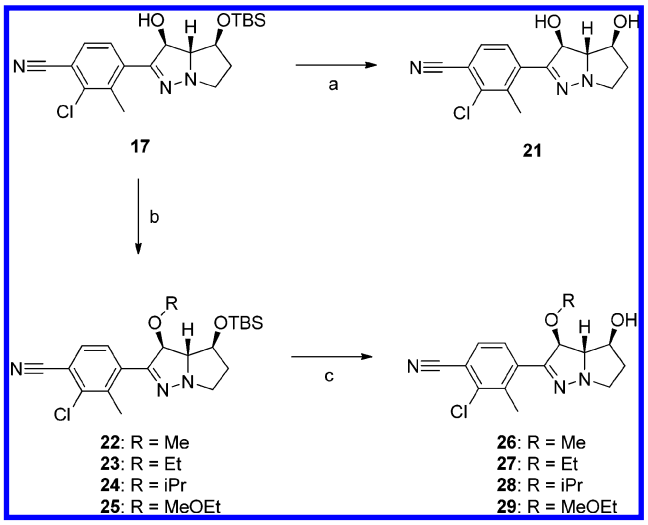

[a]Reagents and conditions: (a) TBAF, THF, 25 °C, 3 h, 28%; (b) exemplary conditions for compound **22**: NaH, iodomethane, THF, 0 °C, 3 h, 82%; (c) exemplary conditions for compound **26**: TBAF, THF, 0 °C, 3 h, 62%.

cocrystallization with the ligand binding domain of the AR (Figure 3), whereby (*S*)-configuration could be assigned to each of the stereocenters.

The free 4-hydroxyl group of **26** could be manipulated in various ways (Scheme 6): inversion of the steric configuration to **30** was accomplished under Mitsunobu conditions, 4-*O*-alkylation to **31** could be completed by deprotonation and treatment with methyl iodide. Fluorination of **30** and **26**, respectively, with DAST afforded **32** and **33.**

Intermediate **20** was methylated (**34**) and treated with TBAF to furnish the 5-hydroxy derivative **35**, which was subjected to inversion of the 5-OH group to give **36**, fluorination to **37**, and oxidation to ketone **38**, which was used to introduce a *gem*-difluoro group into the molecule (**39**) (Scheme 7).

RESULTS AND DISCUSSION

In Vitro Biological Data. Primary agonism of the 3-alkoxy-pyrrolo[1,2-*b*]pyrazolines was measured in an AR reporter gene assay using the murine myoblast cell line C2C12 transiently transfected with human AR and an androgen-specific response-element-driven luciferase reporter gene. Table 1 summarizes potency (EC_{50}) and maximal efficacy relative to DHT (E_{max}) of compounds observed in this assay.

3,4-Diol **21** proved to be a weak, partial AR agonist at low micromolar concentrations only. 3-*O*-Alkylation, however, rendered the compounds highly potent (EC_{50} <5 nM) and fully efficacious (E_{max} ∼100%), as shown for **26**−**28**. Linear alkyl chains were preferred over isopropyl; the solubilizing methoxyethyl chain (**29**) was well-tolerated. Inversion of the hydroxyl group in position 4 (**30**) retained potency (albeit with lower intrinsic efficacy compared to **26**), in contrast to the hydantoin SAR demonstrated previously[31] but in agreement with the imidazolin-2-one SAR reported by Li et al.[27] Docking **30** into the AR ligand binding domain reveals that its 4-OH group is expected to interact only with Asn705 and not Thr877 (Figure 4a), suggesting that the Thr877 interaction may not be essential for biological activity. *O*-methylation in that position (**31**) led to roughly a 13-fold loss of potency. Conversion of the 4-OH group into a fluoro substituent led to the most potent compound of the series (**33**) with an EC_{50} of 0.16 nM, whereas its epimer **32** showed approximately 10-fold lower activity. The docked binding model of **33** (Figure 4b) demonstrates that its fluorine atom is likely to form a halogen bond with Asn705 and Thr877, thereby allowing a binding pocket orientation very similar to that of **26**. A switch of the hydroxyl group from position 4 to 5, conserving the steric configuration, led to a

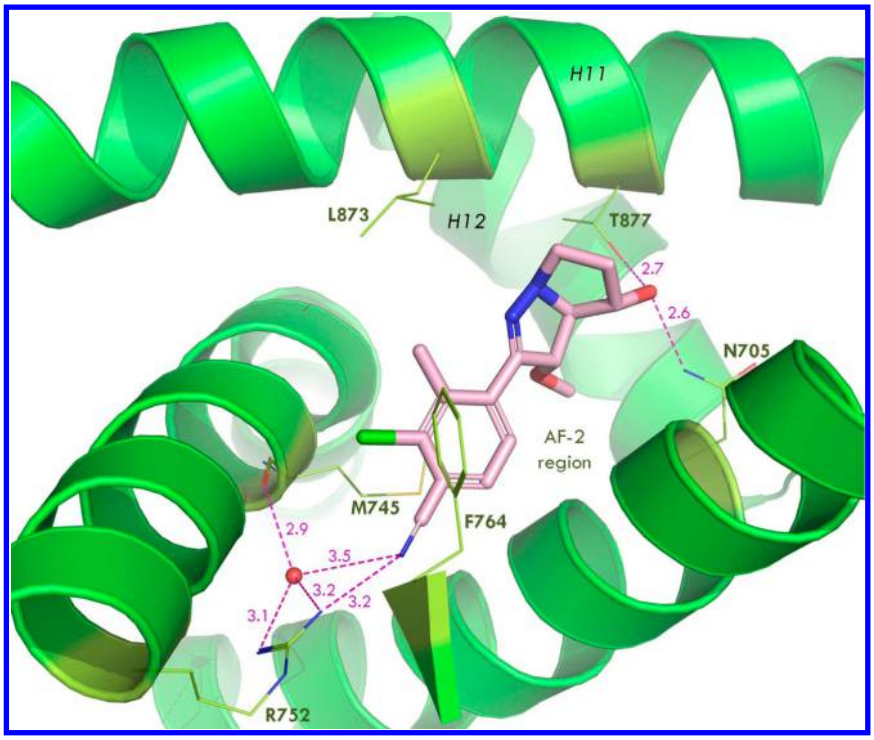

Figure 3. X-ray cocrystal structure of **26** bound to the AR ligand binding domain at 2.1 Å resolution. Key interactions between **26** and residues in the active site are highlighted by dashed lines indicating polar interactions. Numerical values shown for the distances are in Å. The cyano group of **26** interacts with the side chain of R752, whereas the 5-hydroxyl group presumably forms a bifurcated hydrogen bond with N705 and T877. The aryl ring with the chloro and methyl substituents being surrounded by hydrophobic residues makes an edge-to-face π-interaction with F764.

Scheme 6. Inversion of Configuration, Fluorination, and Methylation of 26[a]

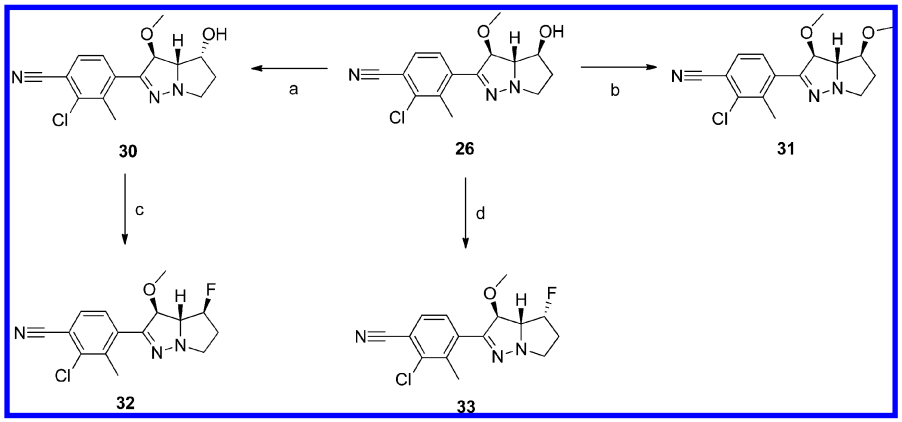

[a]Reagents and conditions: (a) Triphenylphosphine, diisopropyl azodicarboxylate, benzoic acid, THF, 25 °C, 3 h; LiOH, H_2O, 0–25 °C, 18 h, 50%; (b) NaH, iodomethane, THF, 25 °C, 2 h, 20%; (c) DAST, DCM, 0 °C, 2 h, 33%; (d) DAST, DCM, 0 °C, 2 h, 40%.

more than 20-fold decrease in potency (**35**), again accompanied by a decrease in E_{max}. AR activity was completely lost after inversion of the OH-configuration (**36**) but fully restored by replacing the hydroxyl group with a fluorine substituent (**37**). Ketone **38** was moderately active (EC_{50} = 26 nM), and geminal difluoro-substitution in position 5 led to the highly active agonist **39**. The docked binding model of **39** (Figure 4c) suggests that this compound may not interact with the Asn705 side chain but that the geminal difluoro substituent picks up several van der Waals contacts with different hydrophobic residues like Leu701, Leu704, or Phe876. This possibly compensates for the missing Asn705 interaction. Overall, these results suggest that the hydroxyl group of the pyrrolidine ring, which we installed based on the published hydantoin SAR, is not critical for AR agonist activity either in position 4 or 5. The pivotal role of the hydroxyl group, however, in modulating the physicochemical properties in this series will be discussed in the following section.

Skin Permeation Assessment. Some of the most potent and efficacious compounds were selected for assessing their transdermal permeation. First, we determined their thermodynamic aqueous solubility at pH 7.4 and log P (Table 2). Using these two parameters together with molecular weight (MW), skin permeability (K_p) and transdermal flux (calcd J) were predicted according to the Potts and Guy relationship:[32]

$$J\ [\mu g/(h\cdot cm^2)] = Sol_{pH\ 7.4}[\mu g/cm^3] \times K_p[cm/h], \text{ and } \log K_p[cm/h] = -2.7 + 0.71 \log P - 0.0061 MW$$

Scheme 7. Derivatization of Intermediate 20[a]

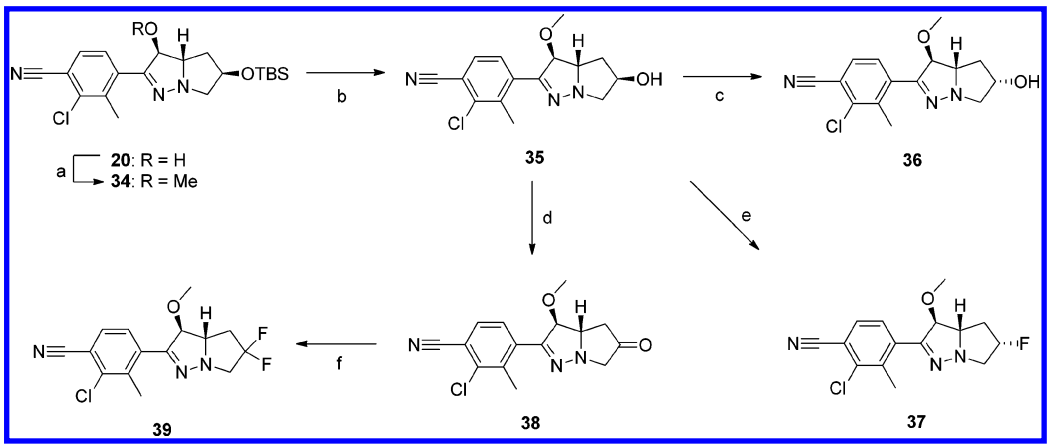

[a]Reagents and conditions: (a) NaH, iodomethane, THF, 25 °C, 2 h, 77%; (b) TBAF, THF, 25 °C, 3 h, 69%; (c) Triphenylphosphine, diisopropyl azodicarboxylate, benzoic acid, THF, 25 °C, 3 h; LiOH, H_2O, 0–25 °C, 18 h, 28%; (d) Dess–Martin periodinane, DCM, 25 °C, 24 h, 86%; (e) DAST, DCM, 0 °C, 2 h, 20%; (f) DAST, DCM, 0 °C, 16 h, 32%.

Table 1. AR Agonist Activity of Derivatives 21–39[a]

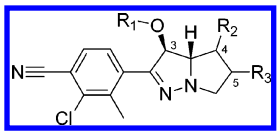

compound	R1	R2	R3	C2C12 EC_{50} [nM]	C2C12 E_{max} [%]
DHT				0.13 ± 0.02	100
21	H	(*S*)-OH	H	978 ± 221	55 ± 21
26	Me	(*S*)-OH	H	0.5 ± 0.4	97 ± 13
27	Et	(*S*)-OH	H	1 ± 0.5	98.3 ± 2.9
28	*i*-Pr	(*S*)-OH	H	4.5 ± 0.1	102 ± 2.8
29	MeOEt	(*S*)-OH	H	0.93 ± 0.3	82 ± 10
30	Me	(*R*)-OH	H	0.4 ± 0.2	86.7 ± 11
31	Me	(*S*)-OMe	H	7.1 ± 1.1	82 ± 4.2
32	Me	(*S*)-F	H	1.5 ± 0.3	93.5 ± 2.1
33	Me	(*R*)-F	H	0.16 ± 0.06	98 ± 3
35	Me	H	(*R*)-OH	9.7 ± 4.2	75 ± 9.5
36	Me	H	(*S*)-OH	inactive	
37	Me	H	(*S*)-F	1.4 ± 0.4	86 ± 19
38	Me	H	O	26 ± 2.4	93 ± 7
39	Me	H	di-F	0.3 ± 0.2	100 ± 0

[a]EC_{50} and E_{max} values are given as the means ± SEM of at least two independent experiments. E_{max} values were determined at 10 μM and were normalized by arbitrarily taking maximal efficacy of DHT as 100%.

However, it should be noted that these estimations are based on aqueous formulations. Thus, changing formulation will change the permeability and solubility of a drug. Furthermore, there is a tendency to overestimate the permeability of ionized and lipophilic compounds. Recently, an in vitro assay was established with artificial membranes consisting of silicone and isopropyl myristate (70:30) that mimic the barrier properties of human stratum corneum, the highest barrier for transdermal drugs.[33,34] This assay is from here onward referred to as "skin-PAMPA" and permits an improved estimation of the passive permeation and distribution of a drug in human skin. In addition, the skin-PAMPA assay allows to discriminate molecules with low membrane retention and low permeation (category A), low membrane retention and high permeation (category B), and high membrane retention and low permeation (category C).

Finally, the most predictive in vitro assay for human skin flux is to measure skin permeation using human cadaver skin in a Franz diffusion cell system.[35] It is the standard in vitro test adopted by the Organisation for Economic Co-operation and Development (OECD) for examining the skin absorption of chemicals.[36] Franz diffusion cells consisting of donor and receptor compartments separated by the skin samples are commonly used for determining the drug permeation in vitro by measuring the amount of drug permeated over time from the donor chamber through the skin and into the acceptor compartment. All studies were performed with saturated aqueous donor solutions in order to maximize drug permeation and allow comparison between compounds.

Below, we are describing the selection of our best SARM candidates using all three methods, as summarized in Table 2.

A thorough analysis of the results shown in Table 2 reveals that compounds **33** and **39**, both devoid of the 4-hydroxy

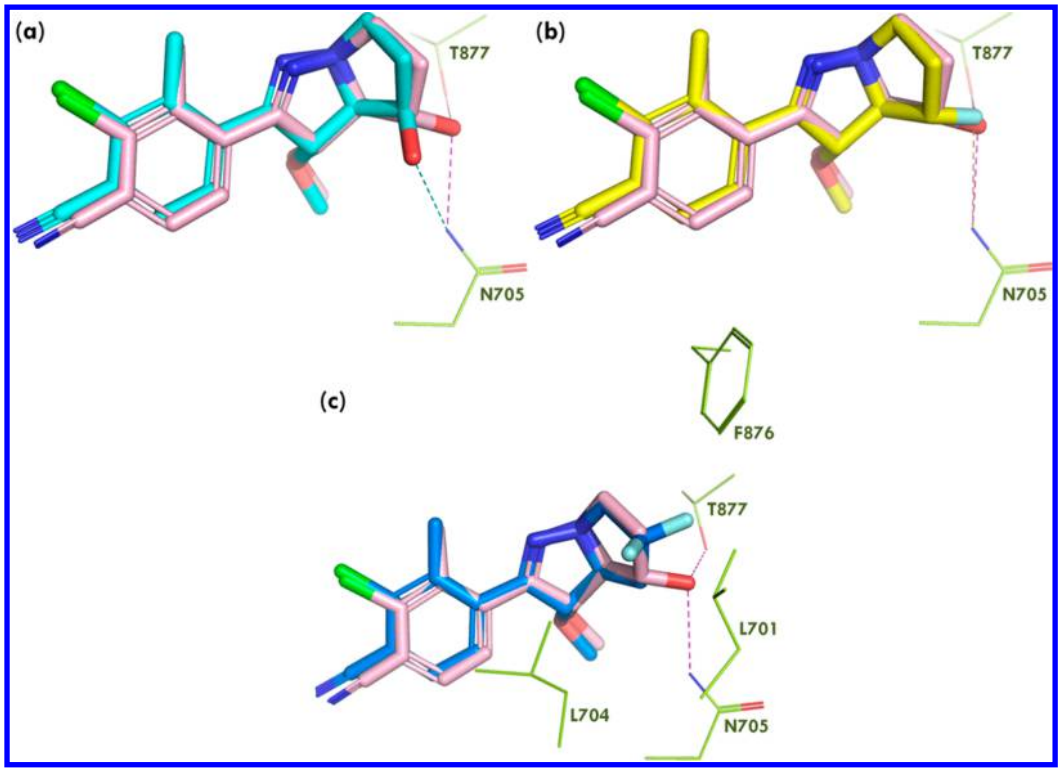

Figure 4. Crystallographic binding mode of **26** (pink) compared with docked models of (a) **30**, (b) **33**, and (c) **39**. Arg752 pocket interactions are not shown.

group, are only poorly soluble in water at neutral pH (Sol = 0.01 mg/mL, respectively). At the same time, they display the highest lipophilicity, as expressed by their measured log *P* values (2.7 and 3.2, respectively). Both parameters are suboptimal for skin permeation (see above), and for the difluoro derivative **39**, this is clearly reflected by the outcome in the skin-PAMPA assay (category C), indicating high membrane retention (due to the highly lipophilic character) and low permeation into the acceptor compartment (due to the lack of solubility). Both compounds rank lowest in the in silico prediction of skin flux (calcd $J < 0.05$ $\mu g/(cm^2 \cdot h)$), and while this was confirmed for **39** in the in vitro Franz cell assay, surprisingly, **33** had a 60-fold higher skin flux in the in vitro assay than predicted. For **33**, the skin-PAMPA assay appeared to be more predictive, as its classification delivered results between B and C, indicating at least moderate permeation.

Gratifyingly, a pyrrolo[1,2-*b*]pyrazoline (**26**) which combined high aqueous solubility (Sol = 1.30 mg/mL) with a very favorable lipophilicity coefficient (log $P = 2.0$) emerged as the molecule with the highest in vitro skin flux at steady state (J_{ss} = 2.0 $\mu g/(cm^2 \cdot h)$) of all tested compounds, exceeding predictions by the in silico method (J_{ss} = 0.85 $\mu g/(cm^2 \cdot h)$) and the skin-PAMPA (category A/B). The exceptionally high aqueous solubility, which exceeds that of **3** by 70-fold, could be attributed to a distinct crystalline form as a mixture of two polymorphs melting at 83 and 89 °C, respectively. Figure 5 demonstrates skin permeation of **26** over time, resulting in a linear cumulation. The observed skin flux at steady state resembles that of known testosterone preparations, where skin permeation enhancers have been used to enhance the systemic bioavailability.[37] Notably, the aqueous formulation of **26** in this experiment was not treated with any permeation enhancer, underlining the high potential of the compound to achieve even higher flux values when using appropriate additives.

Its closest analogue, epimer **30**, was inferior in terms of solubility (Sol = 0.25 mg/mL) and in vitro skin flux (J_{ss} = 0.2 $\mu g/(cm^2 \cdot h)$). 3-*O*-alkyl chain extension by one carbon (**27**) reduced both solubility and in vitro skin flux to some extent, whereas the solubilizing methoxyethyl group of **29** resulted in the highest aqueous solubility measured in this series (Sol = 2.30 mg/mL) but not adequately superior skin flux. It could be clearly concluded that both models of skin permeation prediction, the Guy and Potts algorithm as well as the artificial membrane assay, had their limitations when looking at relatively similar molecules. Only highly lipophilic and poorly soluble compounds such as **39** were correctly classified as weak permeants. Based on the favorable potency and predicted skin permeation potential, **26** emerged as an attractive candidate for additional profiling.

Selectivity of **26** against other nuclear hormone receptors was determined by measuring binding affinity for AR, the glucocorticoid receptor (GR), progesterone receptor (PR), and estrogen receptor (ER). The compound showed high selectivity for AR, as shown in Table 3.

Pharmacokinetics. The pharmacokinetics of the compound with the best predicted and measured flux through human skin, **26**, was analyzed in male Wistar rats using subcutaneous (sc) bolus injection as a surrogate for transdermal systemic delivery. Drug exposure over 24 h was compared to the AUC after intravenous (iv) injection. Results are summarized in Table 4. **26** showed moderate-to-high clearance but high subcutaneous bioavailability, slow absorption from subdermal compartments, and a long elimination half-life after reaching peak plasma concentrations after 1.5 h. This profile was considered highly advantageous, as one could expect a similar exposure-overtime profile from a transdermal patch.

In Vivo Efficacy. **26** was evaluated for efficacy and tissue selectivity in the Hershberger assay.[38] This is a well-established

Table 2. Physicochemical Profiling and in Vitro Skin Permeation[a]

	Cpd	MW	Sol pH 7.4 [mg/mL]	log *P* (oct/water)	skin PAMPA category	calcd J_{ss} [μg/(cm²*h)]	measured J_{ss} [μg/(cm²*h)]
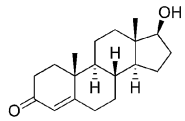	**T**	288.4	0.04	3.3	B	0.27	0.19 ± 0.05
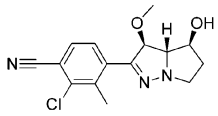	**26**	305.8	1.30	2.0	A/B	0.85	2.0 ± 0.2
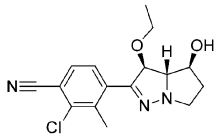	**27**	319.8	0.25	2.4	B	0.26	0.9 ± 0.1
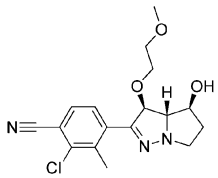	**29**	349.8	2.3	2.0	n.d.	0.81	1.1 ± 0.3
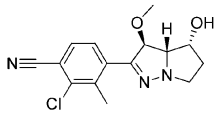	**30**	305.8	0.25	1.9	n.d.	0.10	0.2 ± 0.0
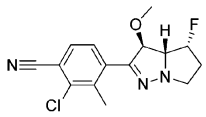	**33**	307.8	0.010	2.7	B/C	0.02	1.2 ± 0.1
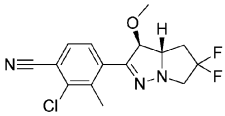	**39**	325.8	0.010	3.2	C	0.04	0.06 ± 0.04

[a]Skin flux values at steady-state (J_{SS}) are given as the means ± SEM of at least three independent experiments. Solubility and log *P* values were determined in single experiments, respectively.

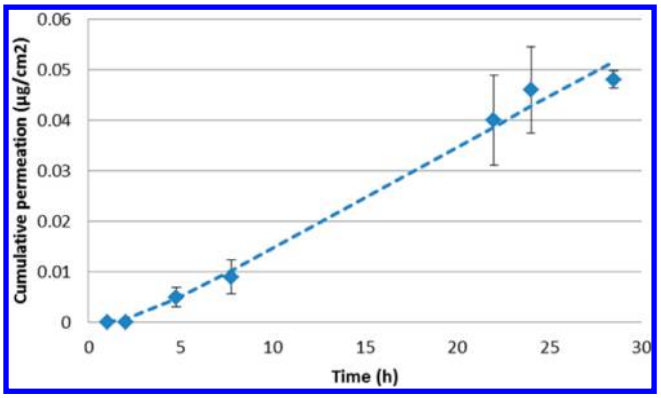

Figure 5. Compound **26** penetrates through human skin from a saturated aqueous solution buffered at pH 7.4. The observed flux at steady state (J_{ss}) is 2.0 ± 0.2 μg/(cm^2·h), based on three different donor skin samples. The dotted line represents the calculated fitted curve using diffusion modeling simulations.

Table 3. Binding Selectivity for 26 in the Nuclear Hormone Receptor Panel[a]

	AR	GR	PR	ER
IC_{50} [nM]	0.7 ± 0.0	>1000	700	>1000

[a]The IC_{50} value for AR is given as the mean ± SEM of two independent experiments, although affinities for GR, PR, and ER were determined in single experiments, respectively.

Table 4. Pharmacokinetics of 26 in Male Wistar Rats

iv injection (1.0 mg/kg)		sc injection (0.5 mg/kg)	
CL [L/h·kg]	1.7	t_{max} [h]	1.5
$t_{1/2}$ [h]	5.7	C_{max} [ng/mL]	79
V_D [L/kg]	4.6	AUC_{0-48} [ng·h/mL]	670
AUC_{0-inf} [ng·h/mL]	708	BAV [%]	75

animal model to assess the anabolic versus androgenic effects of compounds by analyzing weight stimulations of bulbocavernosus/levator ani (BLA) muscle versus prostate in immature orchidectomized (ORX) male rats, respectively. Two weeks after castration, rats were treated with subcutaneous injections of ascending doses of **26** for 14 days. As a control for nonselective androgen action, rats were also treated with a subcutaneous dose range of testosterone propionate (TP). Figure 6 shows dose response curves of **26** and TP on BLA muscle and prostate related to vehicle-treated ORX and sham animals. TP stimulated BLA and prostate weights comparably with very similar ED_{50} values of 0.29 and 0.31 mg/kg, respectively. In contrast, **26** recovered BLA weight much more potently than prostate weight with ED_{50} values of 0.07 and 2.73 mg/kg, respectively. Thus, a window of selective stimulation of muscle versus prostate was observed over two log units of doses from 0.03 to 3 mg/kg with maximal selectivity at 0.3 mg/kg, where muscle was fully restored and prostate only minimally stimulated. Analysis of plasma levels of **26** 3 h after the last administration on day 15 revealed a dose-proportional drug exposure indicating no saturation or accumulation during the 2 week treatment period.

The in vivo efficacy and selectivity of **26** show some resemblance to the profile described for **3**.[26] This may be due to the similarity of the binding modes suggested by the respective X-ray cocrystal structures. It can been speculated whether certain molecular features (e.g., the peripheral hydroxyl group which apparently forms a hydrogen bond with T877) may impact the conformation of the activator function-2 (AF-2) pocket. Such conformational changes are thought to influence the ability of the liganded AR to recruit coactivator and corepressor proteins that show a differential expression pattern in reproductive and anabolic tissues, resulting in different degrees of tissue selectivity in vivo. However, a clear and uniformly accepted link between molecular structure and phenotypic observations has been elusive to date. Continuing efforts in our group are addressing the role of such molecular features, in particular the 4-OH group, in the class of pyrrolo[1,2-*b*]pyrazolines.

■ CONCLUSIONS

This study validated the concept of transdermal drug−likeness applied on a novel class of SARMs using appropriate design parameters, prediction models, and assays. Based on its high potency, selectivity, and efficacy in the Hershberger model, and its ability to permeate through human skin in vitro, **26** holds promise as a novel transdermal AR modulator for the treatment of various muscle wasting disorders potentially avoiding essential limitations of oral SARMs.

■ EXPERIMENTAL SECTION

Chemistry. Unless otherwise stated, all procedures were performed under an argon atmosphere using anhydrous solvents purchased from commercial sources. Commercially available starting materials and reagents were used as received without further purification. Intermediates were characterized

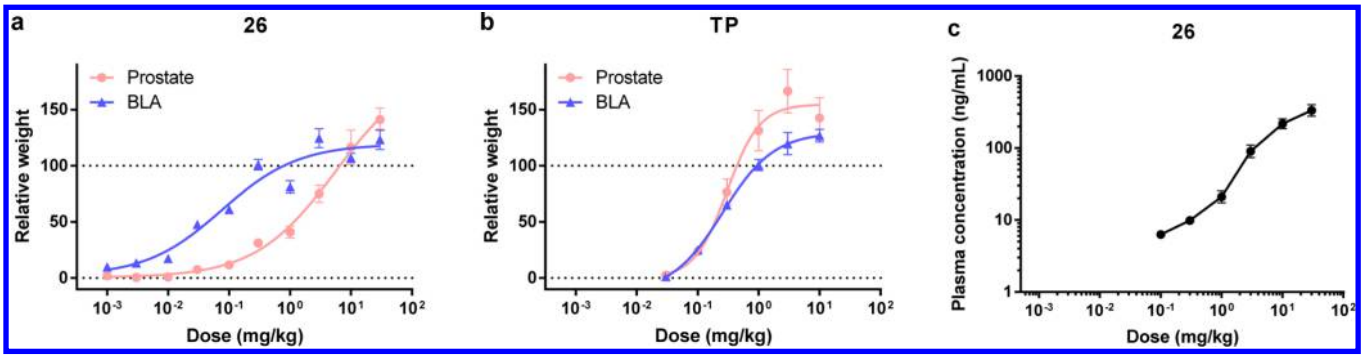

Figure 6. Hershberger in vivo assay of **26**. Dose−response curves of **26** (a) and TP (b) as control for the stimulation of BLA muscle and prostate weights in ORX rats. Relative weights are shown by normalizing to vehicle-treated ORX rats taken as 0% and vehicle-treated Sham rats taken as 100%. (c) Plasma levels of **26** 3 h after the last dosing on day 15.

by electrospray mass spectroscopy (ES-MS) and 1H NMR except when not purified due to the lack of chemical stability and used as crude materials in the subsequent steps (ES-MS only). Final compounds were characterized by melting point, 1H NMR, liquid chromatography/mass spectroscopy (LC/MS) and chiral HPLC with respective retention times (t_R) as well as diasteromeric excess values given. Thin-layer chromatography was performed using precoated Merck silica gel 60 F254 plates, visualized under UV light. Preparative chromatography was conducted over Merck silica gel (0.040−0.063 mm). All ^{1}H NMR spectra were recorded using a Varian Mercury (400 MHz) spectrometer, and samples were dissolved in the deuterated solvents as specified. Chemical shifts are expressed in parts per million as a δ value relative to the shift of tetramethylsilane. Infrared spectra were recorded on a Shimadzu, FT-IR Prestige 21 spectrometer. LC/MS was performed on an Applied Biosciences API-3000 instrument with a photodiode array detector coupled to a mass spectrometer with electrospray ionization. The following HPLC method was chosen: Waters Xterra RP18 (3.5 μm, 50 × 2.1 mm i.d.); (A) water + 0.01% of formic acid and (B) acetonitrile + 0.01% of formic acid; gradient from 95/5 A/B at time 0 to 100% B after 4 min, then 100% B for 3 min. The purity of the described test compounds was at least 95% according to HPLC analysis. Chiral HPLC was performed on a Chiralpak-IA (250 × 4.6 × 5.0 μm) using the following conditions: mobile phase A: *n*-hexane; mobile phase B: ethanol, isocratic: 70:30 (A/B), flow rate: 1.0 mL/min, column temperature: ambient, diluent: ethanol. Monitoring wavelengths are indicated for each compound, and diastereomeric excess (de) values are given. Melting points were measured on a Buchi melting point apparatus B-540, except for **26**, where the melting point was determined by differential scan calorimetry using a TA Instruments Q2000 calorimeter calibrated for temperature and enthalpy with indium (>99.9999% pure).

*(2R,3S)-1-Amino-3-(tert-butyldimethylsilyloxy)pyrrolidin-2-yl)methanol (**8**). Step 1: (2S,3S)-Methyl 3-Hydroxy-1-nitrosopyrrolidine-2-carboxylate (**5**).* To a solution of **4**[26] (16 g, 0.110 mol) in water (60 mL) was added $NaNO_2$ (16 g, 0.220 mol) in water (30 mL) followed by the addition of glacial acetic acid (9.43 mL, 0.165 mol) at 0 °C, and the reaction mixture was stirred for 4 h. Once the starting material had disappeared (monitored by TLC), the reaction mixture was diluted with ethyl acetate. The organic layer was washed with water, brine, dried over Na_2SO_4 and concentrated to obtain 13 g (68%) of the title compound, which was used in the next step without purification. ES-MS: m/z 175 $(M + H)^+$.

*Step 2: (2S,3S)-Methyl 3-(tert-Butyldimethylsilyloxy)-1-nitrosopyrrolidine-2-carboxylate (**6**).* To a solution of **5** (13 g, 0.0742 mol) in DCM (150 mL) at room temperature were added imidazole (15.2 g, 0.224 mol) and TBDMS-Cl (22.5 g, 0.149 mol), and the mixture was stirred at room temperature for 3 h. The reaction mixture was diluted with DCM and washed with water, brine, dried over Na_2SO_4, and concentrated. Purification by column chromatography over silica gel using 10% ethyl acetate in hexane provided 20 g (93%) of the title compound. ^{1}H NMR (400 MHz, DMSO-d_6) (mixture of rotamers): δ 5.19−5.17 (m) and 4.72−4.70 (m, 1H), 4.58−4.54 (m) and 4.17−4.16 (m, 1H), 4.57−4.41 (m, 1H), 3.75(s) and 3.65 (s, 3H), 3.63−3.58 (m, 1H), 2.28−2.23 (m, 1H), 2.10−2.00 (m, 1H), 0.84 (s, 9H), 0.11 (d, J = 4.4 Hz, 3H), 0.07 (d, J = 4.7 Hz, 3H): ES-MS: m/z 289 $(M + H)^+$.

*Step 3: (2R,3S)-3-(tert-Butyldimethylsilyloxy)-1-nitrosopyrrolidin-2-yl)methanol (**7**).* To a solution of **6** (20 g, 0.0692 mol) in THF (350 mL) at −78 °C was added Superhydride (207 mL, 0.207 mol, 1 M solution in THF), and the reaction mixture was stirred at room temperature for 5 h. Then it was poured over ice cold water and extracted with ethyl acetate. The organic layer was washed with water, brine, dried over Na_2SO_4, and concentrated. Purification by column chromatography over silica gel using 30% ethyl acetate in hexane provided 10.5 g (58%) of the title compound. ^{1}H NMR (400 MHz, DMSO-d_6): δ 5.08 (t, J = 5.9 Hz, 1H), 4.43−4.42 (m, 1H), 4.21−4.09 (m, 1H), 3.66−3.59 (m, 2H), 3.57−3.40 (m, 2H), 2.16−2.07 (m, 1H), 1.75−1.72 (m, 1H), 0.76 (s, 9H), 0.03 (s, 3H), 0.02 (s, 3H) ; IR (KBr): 3309, 2953, 2929, 2858, 1469 cm^{-1}; ES-MS: m/z 261 $(M + H)^+$.

*Step 4: (2R,3S)-1-Amino-3-(tert-Butyldimethylsilyloxy)-pyrrolidin-2-yl)methanol (**8**).* To a solution of **7** (9.0 g, 0.034 mol) in methanol (140 mL) at room temperature were added zinc dust (23 g, 0.353 mol) and NH_4Cl (28 g, 0.529 mol). After the addition was over, water (70 mL) was added at 0 °C and the reaction mixture was stirred at room temperature for 30 min and then at 50 °C for 1 h. Once the starting material had disappeared (monitored by TLC), the reaction mixture was cooled to room temperature, filtered, and the filtrate was concentrated to give a liquid which was diluted with ethyl acetate. Organic layer was washed with water, brine, dried over Na_2SO_4 and concentrated to obtain 7 g (83%) of the title compound, which was not stable enough to conduct NMR or LC data. The material was used with MS characterization only and without further purification to prepare compound **15**. ES-MS: m/z 247 $(M + H)^+$.

*(2S,4R)-1-Amino-4-(tert-Butyldimethylsilyloxy)pyrrolidin-2-yl)methanol (**13**). Step 1: (2S,4R)-Methyl 4-Hydroxy-1-nitrosopyrrolidine-2-carboxylate (**10**).* To a solution of **9**[39] (55.2 g, 0.381 mol) in water (350 mL) was added $NaNO_2$ (52.5 g, 0.762 mol) in water (150 mL) followed by the addition of glacial acetic acid (34.3 mL, 0.571 mol) at 0 °C, and the reaction mixture was stirred for 4 h. Once the starting material disappeared (monitored by TLC), the reaction mixture was diluted with ethyl acetate. The organic layer was washed with water, brine, dried over Na_2SO_4, and concentrated to get 66.3 g (100%) of the title compound, which was used in the next step without purification. ES-MS: m/z 175 $(M + H)^+$.

*Step 2: (2S,4R)-Methyl 4-(tert-Butyldimethylsilyloxy)-1-nitrosopyrrolidine-2-carboxylate (**11**).* To a solution of **10** (66 g, 0.381 mol) in DCM (1.3 L) at room temperature were added imidazole (77.7 g, 1.143 mol) and TBDMS-Cl (115 g, 0.762 mol) and the mixture was stirred at room temperature for 3 h. The reaction mixture was diluted with DCM and washed with water, brine, dried over Na_2SO_4 and concentrated. Purification by column chromatography over silica gel using 10% ethyl acetate in hexane provided 95 g (87%) of the title compound. ^{1}H NMR (400 MHz, DMSO-d_6): δ 4.64−4.54 (m, 1H), 4.43 (t, J = 8.83 Hz, 1H), 4.30−4.38 (m, 2H), 3.62 (s, 3H), 2.23−2.17 (m, 2H), 0.84 (s, 9H), 0.07(s, 6H); ES-MS: m/z 289 $(M + H)^+$.

*Step 3: (2S,4R)-4-(tert-Butyldimethylsilyloxy)-1-nitrosopyrrolidin-2-yl)methanol (**12**).* To a solution of **11** (20g, 0.069 mol) in THF (400 mL) at −78 °C was added Superhydride (207 mL, 0.207 mol, 1 M solution in THF) and stirred at room temperature for 5 h. The reaction mixture was poured over ice cold water and extracted with ethyl acetate. The organic layer was washed with water, brine, dried over Na_2SO_4, and

concentrated. Purification by column chromatography over silica gel using 30% ethyl acetate in hexane provided 12g (67%) of the title compound. ^{1}H NMR (400 MHz, DMSO-d_6): δ 5.0 (m, 1H), 4.59−4.55 (m, 2H), 3.89−3.88 (m, 1H), 3.81−3.79 (m, 1H), 3.55−3.49 (m, 2H), 2.24−2.19 (m, 1H), 2.05−2.02 (m, 1H), 0.84 (s, 9H), 0.07 (s, 6H); ES-MS: m/z 261 (M + H)$^+$.

Step 4: (2S,4R)-1-Amino-4-(tert-Butyldimethylsilyloxy)-pyrrolidin-2-yl)methanol (13). To a solution of **12** (12 g, 0.046 mol) in methanol (120 mL) at room temperature were added zinc dust (30.5 g, 0.46 mol) and NH_4Cl (36.4 g, 0.69 mol). After the addition was over, water (60 mL) was added at 0 °C, and the reaction mixture was stirred at room temperature for 30 min and then at 50 °C for 1 h. Once the starting material disappeared (monitored by TLC), the reaction mixture was cooled to room temperature, filtered, and the filtrate was concentrated to give a liquid which was diluted with ethyl acetate. The organic layer was washed with water, brine, dried over Na_2SO_4, and concentrated to get 11 g (97%) of the title compound, which was not stable enough to conduct NMR or LC data. The material was used with MS characterization only and without further purification to prepare compound **18**. ES-MS: m/z 247 (M + H)$^+$.

2-Chloro-4-formyl-3-methylbenzonitrile (14).[26,28] Modified procedure: To a stirred solution of 2-chloro-4-iodo-3-methylbenzonitrile in dry THF at 0 °C was added isopropyl magnesium chloride (14.5 mL, 129.7 mmol, 2 M solution in ether) dropwise, and the reaction mixture was stirred for 2 h at 0 °C. To this, 1-formyl piperidine (64.8 mL, 129.7 mmol) was added at 0 °C and stirred at same temperature for 2 h. The reaction mixture was quenched with saturated NH_4Cl solution and extracted with ethyl acetate. The organic layer was washed with water, brine, dried over Na_2SO_4, and concentrated. The crude product was purified by column chromatography using 8% ethyl acetate in hexane as eluent to give 14.5 g (75%) of the title compound. ^{1}H NMR (400 MHz, DMSO-d_6): δ 10.32 (s, 1H), 8.03 (d, J = 8.2 Hz, 1H), 7.92 (d, J = 8.2 Hz, 1H), 2.71 (s, 3H); IR (KBr): 3072, 2962, 2927, 2856, 2237, 1707 cm^{-1}.

4-((*E*)-((2*R*,3*S*)-3-(*tert*-Butyldimethylsilyloxy)-2-(hydroxymethyl)pyrrolidin-1-ylimino)methyl)-2-chloro-3-methylbenzonitrile (15). A mixture of **8** (7 g, 0.028 mol) and **14** (5.6 g, 0.0313 mol) in glacial acetic acid (60 mL) was stirred at room temperature for 3 h. Once both the starting materials disappeared (monitored by TLC), the reaction mixture was poured into ice water and extracted with ethyl acetate. The organic layer was washed with water, brine, dried over Na_2SO_4, and concentrated to give crude product which was purified by column chromatography over silica gel using 15% ethyl acetate in hexane as a solvent to provide 7.5 g (66%) of the title compound. ^{1}H NMR (400 MHz, DMSO-d_6): δ 7.77 (d, J = 8.3 Hz, 1H), 7.65 (d, J = 8.8 Hz, 1H), 7.20 (s, 1H), 4.87−4.85 (m, 1H), 4.38 (s, 1H), 3.61−3.59 (m, 1H), 3.58−3.41 (m, 3H), 3.29−3.24 (m, 1H), 2.44 (s, 3H), 2.23−2.08 (m, 1H), 1.89−1.85 (m, 1H), 0.85 (s, 9H), 0.09 (s, 3H), 0.08 (s, 3H) ; IR (KBr): 3473, 2945, 2854, 2233, 1522, 1523 cm^{-1}; ES-MS: m/z 408 (M + H)$^+$.

4-((*E*)-((2*S*,3*S*)-3-(*tert*-Butyldimethylsilyloxy)-2-formyl-pyrrolidin-1-ylimino)methyl)-2-chloro-3-methylbenzonitrile (16). To a solution of oxalyl chloride (1.92 mL, 0.022 mol) in dry DCM (25 mL) at −78 °C was added DMSO (3.12 mL, 0.044 mol), and the mixture was stirred for 30 min. Then a solution of **15** (7.5 g, 0.0184 mol) in 100 mL DCM was added at the same temperature and stirring continued for 1 h. The reaction mixture was quenched with triethylamine (13 mL) at −30 °C and stirred for 1 h. Then it was diluted with DCM and washed with water, brine, dried over Na_2SO_4, and concentrated to get 7.0 g (94%) of the title compound which was used in the next step without further purification. ^{1}H NMR (400 MHz, DMSO-d_6): δ 9.53 (d, J = 1.9 Hz, 1H), 7.62 (d, J = 8.3 Hz, 1H), 7.57 (d, J = 8.3 Hz, 1H), 7.29 (s, 1H), 4.52−4.51 (m, 1H), 4.01 (s, 1H), 3.60−3.53 (m, 1H), 3.37−3.17 (m, 1H), 2.36 (s, 3H), 2.10−2.05 (m, 1H), 1.89−1.85 (m, 1H), 0.76 (s, 9H), 0.009 (s, 3H), 0.00 (s, 3H); IR (KBr): 2953, 2927, 2856, 2227, 1730, 1556 cm^{-1}; EC-MS: m/z 406 (M + H)$^+$.

4-((3*S*,3a*R*,4*S*)-4-(*tert*-Butyldimethylsilyloxy)-3-hydroxy-3a,4,5,6-tetrahydro-3H-pyrrolo[1,2-*b*]pyrazol-2-yl)-2-chloro-3-methylbenzonitrile (17). To a solution of **16** (7.0 g, 0.0172 mol) in DCM (100 mL) at 0 °C was added borontrifluoride diethyl etherate (6.2 mL, 0.0207 mol), and the reaction mixture was stirred at room temperature for 3 h. Once the starting material had disappeared (monitored by TLC), the reaction mixture was diluted with DCM, water and washed with saturated $NaHCO_3$ aqueous solution, water, brine, dried over Na_2SO_4, and concentrated to get the crude product. Purification of the crude by column chromatography over silica gel using 10% ethyl acetate in hexane as a solvent provided 4.2 g (60%) of the title compound. ^{1}H NMR (400 MHz, DMSO-d_6): δ 7.87 (d, J = 8.3 Hz, 1H), 7.71 (d, J = 8.3 Hz, 1H), 5.94 (d, J = 6.8 Hz, 1H), 5.27 (d, J = 7.3 Hz, 1H), 4.17−4.15 (m, 1H), 3.55−3.50 (m, 1H), 3.45−3.42 (m,1H), 3.41−3.40 (m, 1H), 2.54 (s, 3H), 1.81−1.76 (m, 1H), 1.62−1.57 (m, 1H), 0.89 (s, 9H), 0.10 (s, 3H), 0.08 (s, 3H); EC-MS: m/z 406 (M + H)$^+$.

4-((E)-((2*S*,4*R*)-4-(*tert*-Butyldimethylsilyloxy)-2-(hydroxymethyl)pyrrolidin-1-ylimino)methyl)-2-chloro-3-methylbenzonitrile (18). A mixture of **13** (11 g, 0.044 mol) and **14** (4 g, 0.022 mol) in glacial acetic acid (60 mL) was stirred at room temperature for 3 h. Once both starting materials disappeared (monitored by TLC), the reaction mixture was poured into ice water and extracted with ethyl acetate. The organic layer was washed with water, brine, dried over Na_2SO_4, and concentrated to give crude product which was purified by column chromatography over silica gel using 15% ethyl acetate in hexane as a solvent to provide 8 g (44%) of the title compound. ^{1}H NMR (400 MHz, DMSO-d_6): δ 7.77 (d, J = 8.3 Hz, 1H), 7.64 (d, J = 9 Hz, 1H), 7.17 (s, 1H), 4.71−4.63 (m, 1H), 4.59 (bs, 1H), 3.82 (bs, 1H), 3.68−3.65 (m, 1H), 3.64−3.61 (m, 2H), 3.11 (d, J = 3.4 Hz, 1H), 2.49 (s, 3H), 2.10−2.06 (m, 1H), 1.90−1.86 (m, 1H), 0.86 (s, 9H), 0.09 (s, 6H); EC-MS: m/z 408 (M + H)$^+$.

4-((E)-((2*S*,4*R*)-4-(*tert*-Butyldimethylsilyloxy)-2-formyl-pyrrolidin-1-ylimino)methyl)-2-chloro-3-methylbenzonitrile (19). To a solution of oxalyl chloride (1.99 mL, 0.022 mol) in dry DCM (60 mL) at −78 °C was added DMSO (3.33 mL, 0.047 mol) and stirred for 30 min. Then a solution of **18** (8 g, 0.019 mol) in 100 mL DCM was added to the reaction mixture at the same temperature, and stirring continued for 1 h. The reaction mixture was quenched with triethylamine (13. mL 0.095 mol) at −30 °C and stirred for 1 h. Then it was diluted with DCM and washed with water, brine, dried over Na_2SO_4, and concentrated to get 8 g (100%) of the title compound which was used in the next step without further purification. Due to the low stability of the product no analytical data was recorded.

4-((3*S*,3a*S*,5*R*)-5-(*tert*-Butyldimethylsilyloxy)-3-hydroxy-3a,4,5,6-tetrahydro-3H-pyrrolo[1,2-*b*]pyrazol-2-

yl)-2-chloro-3-methylbenzonitrile (20). To a solution of **19** (8 g, 0.019 mol) in DCM (160 mL) at 0 °C was added borontrifluoride diethyl etherate (2.9 mL, 0.024 mol), and the reaction mixture was stirred at room temperature for 3 h. Once the starting material disappeared (monitored by TLC), the reaction mixture was diluted with DCM, water and washed with saturated aqueous $NaHCO_3$ solution, water, brine, dried over Na_2SO_4, and concentrated to get the crude product. Purification of the crude material was achieved by column chromatography over silica gel using 10% ethyl acetate in hexane as a solvent provided 4 g (50%) of the title compound. ^{1}H NMR (400 MHz, DMSO-d_6): δ 7.85 (d, J = 8.3 Hz, 1H), 7.70 (d, J = 8.3 Hz,1H), 5.78 (d, J = 6.3 Hz, 1H), 5.10 (d, J = 6.3 Hz, 1H), 4.39−4.37 (m, 1H), 3.84−3.80 (m, 1H), 3.69−3.65 (m, 1H), 3.20−3.16 (m, 1H), 2.54 (s, 3H), 1.73−1.72 (m, 1H), 1.64−1.61 (m, 1H), 0.86 (s, 9H), 0.05 (s, 6H); ES-MS: m/z 406 (M + H)$^+$.

2-Chloro-4-((3*S*,3a*S*,4*S*)-3,4-dihydroxy-3a,4,5,6-tetrahydro-3H-pyrrolo[1,2-*b*]pyrazol-2-yl)-3-methylbenzonitrile 21). To a solution of **17** (50 mg, 0.1233 mmol) in THF (2 mL) at 0 °C was added tetrabutylammonium fluoride (0.24 mL, 0.246 mmol, 1 M solution in THF), and the reaction mixture was stirred at room temperature for 3 h. Once the starting material had disappeared (monitored by TLC), it was diluted with ethyl acetate and washed with water, brine, dried over Na_2SO_4, and concentrated. Purification by column chromatography over silica gel using 3% methanol in DCM as solvent provided 10 mg (28%) of the title compound, mp 163 °C. ^{1}H NMR (400 MHz, DMSO-d_6): δ 7.85 (d, J = 8.2 Hz, 1H), 7.69 (d, J = 8.2 Hz, 1H), 5.87 (d, J = 6.7 Hz, 1H), 5.26 (d, J = 6.4 Hz, 1H), 5.15 (d, J = 4.2 Hz, 1H), 3.93−3.80 (m, 1H), 3.48−3.43 (m, 2H), 3.40−3.34 (m, 1H), 2.53 (s, 3H), 1.81−1.74 (m, 1H), 1.62−1.61 (m, 1H); IR (KBr): 3442, 3363, 2951, 2239, 1587, 1568 cm^{-1}; LC/MS (t_R = 1.91 min): m/z 292 (M + H)$^+$; chiral HPLC (wavelength 238 nm): t_R = 8.42 min, de = 97%.

4-((3*S*,3a*R*,4*S*)-4-(*tert*-Butyldimethylsilyloxy)-3-methoxy-3a,4,5,6-tetrahydro-3H-pyrrolo[1,2-*b*]pyrazol-2-yl)-2-chloro-3-methylbenzonitrile (22). To a solution of **17** (500 mg, 1.234 mmol) in THF (10 mL) at 0 °C was added NaH (99 mg, 1.851 mmol), and the reaction mixture was stirred for 30 min. Methyl iodide (0.11 mL, 2.469 mmol) was added to the reaction mixture at 0 °C and it was stirred at room temperature for 3 h. The reaction mixture was poured over ice cold water and extracted with ethyl acetate. The organic layer was washed with water, brine, dried over Na_2SO_4, and concentrated. Purification by column chromatography over silica gel using 10% ethyl acetate in hexane provided 0.42 g (82%) of the title compound. ^{1}H NMR (400 MHz, DMSO-d_6): δ 7.88 (d, J = 7.8 Hz, 1H), 7.68 (d, J = 8.3 Hz, 1H), 5.20 (s, 1H), 4.16 (q, J = 4.9 Hz,1H), 3.55−3.45 (m, 3H), 3.22 (s, 3H), 2.55 (s, 3H), 1.88−1.81 (m, 1H), 1.69−1.62 (m, 1H), 0.89 (s, 9H), 0.11 (s, 3H), 0.09 (s, 3H) ; EC-MS: m/z 420 (M + H)$^+$.

4-((3*S*,3a*R*,4*S*)-4-(*tert*-Butyldimethylsilyloxy)-3-ethoxy-3a,4,5,6-tetrahydro-3H-pyrrolo[1,2-*b*]pyrazol-2-yl)-2-chloro-3-methylbenzonitrile (23). The title compound was prepared according to the procedure for **22**, replacing methyl iodide with ethyl iodide, to give 72 mg (67%) of product. ^{1}H NMR (400 MHz, $CDCl_3$): δ 7.54−7.48 (m, 2H), 5.00 (d, J = 1.5 Hz, 1H), 3.91−3.89 (m, 1H), 3.69−3.63 (m, 3H), 3.53−3.43 (m, 2H), 2.61 (s, 3H), 2.02−1.90 (m, 1H), 1.82−1.79 (m, 1H), 1.18 (t, J = 6.8 Hz, 3H), 0.91 (s, 9H), 0.09 (s, 3H), 0.08 (s, 3H); EC-MS: m/z 434 (M + H)$^+$.

4-((3*S*,3a*R*,4*S*)-4-(*tert*-Butyldimethylsilyloxy)-3-isopropoxy-3a,4,5,6-tetrahydro-3H-pyrrolo[1,2-*b*]pyrazol-2-yl)-2-chloro-3-methylbenzonitrile (24). The title compound was prepared according to the procedure for **22**, replacing methyl iodide with isopropyl iodide, to give 18 mg (16%) of product. ^{1}H NMR (400 MHz, $CDCl_3$): δ 7.52 (d, J = 7.9 Hz, 1H), 7.43 (d, J = 8.3 Hz, 1H), 4.99 (s, 1H), 3.89−3.86 (m, 1H), 3.71−3.67 (m, 2H), 3.65−3.58 (m, 2H), 2.59 (s, 3H), 2.04−2.00 (m, 1H), 1.84−1.79 (m, 1H), 1.18 (d, J = 5.9 Hz, 3H), 1.13 (d, J = 5.9 Hz, 3H), 0.91 (s, 9H), 0.09 (s, 3H), 0.08 (s, 3H); EC-MS: m/z 448 (M + H)$^+$.

4-((3*S*,3a*R*,4*S*)-4-(*tert*-Butyldimethylsilyloxy)-3-(2-methoxyethoxy-3a,4,5,6-tetrahydro-3H-pyrrolo[1,2-*b*]-pyrazol-2-yl)-2-chloro-3-methylbenzonitrile (25). To a suspension of sodium hydride (99 mg, 2.5 mmol) in THF (5 mL) at 0 °C was added a solution of **17** (500 mg, 1.2 mmol) in THF (10 mL) and stirred for 10 min, followed by the addition of 1-bromo-2-methoxyethane (0.14 mL, 1.5 mmol). The reaction mixture was stirred at 70 °C for 5 h. Once the starting material had disappeared (monitored by TLC), the reaction was cooled and quenched with saturated ammonium chloride solution, and extracted with ethyl acetate. The organic layer was washed with water, brine, dried over Na_2SO_4, and concentrated. Purification by column chromatography (silica gel, 10% ethyl acetate in Hexane) provided the title compound (500 mg, 87%). ^{1}H NMR (400 MHz, $CDCl_3$): δ 7.59 (d, J = 7.8 Hz, 1H), 7.53 (d, J = 8.3 Hz, 1H), 5.15 (d, J = 1.0 Hz, 1H), 3.91−3.89 (m, 1H), 3.68−3.64 (m, 3H), 3.58−3.50 (m, 2H), 3.49−3.47 (m, 2H), 3.32 (s, 3H), 2.62 (s, 3H), 1.96−1.94 (m, 1H), 1.81−1.80 (m, 1H), 0.91 (s, 9H), 0.09 (d, J = 5.3 Hz, 6H); EC-MS: m/z 464 (M + H)$^+$.

2-Chloro-4-((3*S*,3a*S*,4*S*)-4-hydroxy-3-methoxy-3a,4,5,6-tetrahydro-3H-pyrrolo[1,2-*b*]pyrazol-2-yl)-3-methylbenzonitrile (26). To a solution of **22** (400 mg, 0.954 mmol) in THF (10 mL) at 0 °C was added tetrabutylammonium fluoride (1.91 mL, 1.91 mmol, 1 M solution in THF), and the reaction mixture was stirred at room temperature for 3 h. Once the starting material had disappeared (monitored by TLC), the reaction mixture was diluted with ethyl acetate and the organic layer was washed with water, brine, dried over Na_2SO_4 and concentrated to give crude product. The material was purified by column chromatography over silica gel using 2% methanol in DCM to provide 190 mg (62%) of the title compound. ^{1}H NMR (400 MHz, $CDCl_3$ + DMSO-d_6): δ 7.53−7.37 (m, 2H), 5.09 (s, 1H), 4.68 (d, J = 4.5 Hz, 1H), 3.99−3.95 (m, 1H), 3.66−3.65 (m, 3H), 3.31 (s, 3H), 2.61 (s, 3H), 2.58 (s, 1H), 2.05−1.95 (m, 1H), 1.90−1.82 (m, 1H); IR (KBr): 3387, 3311, 3234, 2933, 2821, 2231, 1589 cm^{-1}; LC/MS (t_R = 2.11 min): m/z 306 (M + H)$^+$; chiral HPLC (wavelength 325 nm): t_R = 6.84 min, de = 99%. Differential scan calorimetry: 0.5 mg of **26** was accurately weighed into a closed sample pan; the temperature of the apparatus was adjusted to −40 °C and heated to 300 °C at a rate of 10 K/min under a nitrogen flow of 50 mL/min. The thermogram showed the presence of two polymorphs, melting at 83 and 89 °C, respectively.

2-Chloro-4-((3*S*,3a*S*,4*S*)-4-hydroxy-3-ethoxy-3a,4,5,6-tetrahydro-3H-pyrrolo[1,2-*b*]pyrazol-2-yl)-3-methylbenzonitrile (27). The title compound was prepared according to the procedure for **26**, using intermediate **23**, to give 30 mg (56%) of product, mp 71 °C. ^{1}H NMR (400 MHz, DMSO-d_6): δ 7.86 (d, J = 8.3 Hz, 1H), 7.65 (d, J = 8.3 Hz, 1H), 5.26−5.21 (m, 2H), 3.94 (bs, 1H), 3.50−3.40 (m, 5H), 2.54 (s, 3H), 1.83−1.78 (m, 1H), 1.67−1.65 (m, 1H), 1.07 (t, J = 6.9 Hz,

3H); IR (KBr): 3180, 2951, 2233, 1589, 1384, 1089 cm^{-1}; LC/MS (t_R = 2.19 min): m/z 320 (M + H)$^+$; chiral HPLC (wavelength 326 nm): t_R = 5.44 min, de = 97%.

2-Chloro-4-((3*S*,3a*S*,4*S*)-4-hydroxy-3-isopropoxy-3a,4,5,6-tetrahydro-3H-pyrrolo[1,2-*b*]pyrazol-2-yl)-3-methylbenzonitrile (28). The title compound was prepared according to the procedure for **26**, using intermediate **24**, to give 5 mg (43%) of product, mp 118 °C. ^{1}H NMR (400 MHz, DMSO-d_6): δ 7.53 (d, J = 8.4 Hz, 1H), 7.45 (d, J = 7.8 Hz, 1H), 5.08 (s, 1H), 4.09 (bs, 1H), 3.75−3.66 (m, 4H), 2.58 (s, 3H), 2.07−2.01 (m, 1H), 1.85−1.80 (m, 1H), 1.78 (bs, 1H), 1.18 (d, J = 6.3 Hz, 3H), 1.14 (d, J = 5.9 Hz, 3H); LC/MS (t_R = 2.25 min): m/z 334 (M + H)$^+$; chiral HPLC (wavelength 326 nm): t_R = 4.45 min, de = 98%.

2-Chloro-4-((3*S*,3a*S*,4*S*)-4-hydroxy-3-(2-methoxyethoxy)-3a,4,5,6-tetrahydro-3H-pyrrolo[1,2-*b*]pyrazol-2-yl)-3-methylbenzonitrile (29). The title compound was prepared according to the procedure for **26**, using intermediate **25**, to give 10 mg (27%) of product, mp =87 °C. ^{1}H NMR (400 MHz, DMSO-d_6): δ 7.58−7.52 (m, 2H), 5.25 (d, J = 1.0 Hz, 1H), 4.10−4.00 (m, 1H), 3.72−3.65 (m, 4H), 3.57−3.51 (m, 3H), 3.34 (s, 3H), 2.61 (s, 3H), 2.05−2.00 (m, 2H), 1.85−1.80 (m, 1H); IR (KBr): 3304, 3219, 2922, 2881, 2852, 2231, 1591 cm^{-1}; LC/MS (t_R = 2.12 min): m/z 350 (M + H)$^+$; chiral HPLC (wavelength 328 nm): t_R = 8.15 min, de =99%.

2-Chloro-4-((3*S*,3a*S*,4*R*)-4-hydroxy-3-methoxy-3a,4,5,6-tetrahydro-3H-pyrrolo[1,2-*b*]pyrazol-2-yl)-3-methylbenzonitrile (30). To a solution of **26** (60 mg, 0.196 mmol) in THF (2 mL) were added triphenylphosphine (77 mg, 0.295 mmol), benzoic acid (36 mg, 0.295 mmol), and diisopropyl azodicarboxylate (0.05 mL, 0.295 mmol), and the reaction mixture was stirred at room temperature for 3 h. Once the starting material had disappeared (monitored by TLC), the reaction mixture was diluted with ethyl acetate. The organic layer was washed with saturated $NaHCO_3$ solution, water and brine, dried over Na_2SO_4, and concentrated to give the benzoate intermediate, which was dissolved in THF (2 mL). At 0 °C a solution of LiOH·H_2O (25 mg, 0.586 mmol) in water was added and the reaction mixture was stirred at room temperature overnight. Once the starting material had disappeared (monitored by TLC), the reaction mixture was extracted with ethyl acetate. The organic layer was washed with saturated $NaHCO_3$ solution, water and brine, dried over Na_2SO_4, and concentrated. Purification of the crude material by column chromatography over silica gel using 2% methanol in DCM provided 30 mg (50%) of the title compound, mp 136 °C. ^{1}H NMR (400 MHz,$CDCl_3$ + DMSO-d_6): δ 7.52 (bs, 2H), 5.39 (d, J = 1.4 Hz, 1H), 4.54−4.50 (m, 1H), 3.79−3.70 (m, 1H), 3.68−3.64 (m, 1H), 3.57−3.51 (m, 1H), 3.26 (s, 3H), 2.61 (s, 3H), 2.19−2.1 (m, 1H), 1.91−1.87 (m, 1H), 1.86 (d, J = 4.9 Hz, 1H); IR (KBr): 3450, 2935, 2231, 1589 cm^{-1}; LC/MS (t_R = 2.10 min): m/z 306 (M + H)$^+$; chiral HPLC (wavelength 328 nm): t_R = 7.55 min, de = 99%.

2-Chloro-4-((3S,3aS,4S)-3,4-dimethoxy-3a,4,5,6-tetrahydro-3H-pyrrolo[1,2-*b*]pyrazol-2-yl)-3-methylbenzonitrile (31). To a stirred solution of **26** (50 mg, 0.16 mmol) in THF (3 mL) at 0 °C was added sodium hydride (13 mg, 0.33 mmol) for 10 min, followed by the addition of methyl iodide (0.015 mL, 0.245 mmol). The reaction mixture was stirred at room temperature for 2 h. Once the starting material had disappeared (monitored by TLC) the reaction mixture was quenched with saturated NH_4Cl solution and extracted with ethyl acetate. The organic layer was washed with water, brine, dried over Na_2SO_4, and concentrated. Purification by column chromatography (silica gel, 30% ethyl acetate in hexane) provided 10 mg (20%) of the title compound, mp 85 °C. ^{1}H NMR (400 MHz, $CDCl_3$): δ 7.55−7.49 (m, 2H), 5.08 (d, J = 1.0 Hz, 1H), 5.50 (d, J = 1.0 Hz, 1H), 3.77−3.73 (m, 2H), 3.66−3.65 (m, 1H), 3.59−3.53 (m, 1H), 3.39 (s, 3H), 3.32 (s, 3H), 2.61 (s, 3H), 1.88−1.84 (m, 2H); LC/MS (t_R = 2.41 min): m/z 320 (M + H)$^+$; chiral HPLC (wavelength 321 nm): t_R = 9.41 min, de = 98%.

2-Chloro-4-((3*S*,3a*R*,4*S*)-4-fluoro-3-methoxy-3a,4,5,6-tetrahydro-3H-pyrrolo[1,2-*b*]pyrazol-2-yl)-3-methylbenzonitrile (32). To a solution of **30** (30 mg, 0.0983 mmol) in DCM (2 mL) at 0 °C was added DAST (0.02 mL, 0.1475 mmol), and the reaction mixture was stirred at same temperature for 2 h. Once the starting material had disappeared (monitored by TLC), the reaction mixture was diluted with DCM, water, and extracted. The organic layer was washed with water, brine, dried over Na_2SO_4, and concentrated. Purification by preparative TLC (40% ethyl acetate in hexane) provided 5 mg (33%) of the title compound as a viscous liquid. ^{1}H NMR (400 MHz, $CDCl_3$): δ 7.55−7.48 (m, 2H), 5.12 (s, 1H), 5.02 (dd, J = 5.3 Hz, 53.7 Hz, 1H), 3.99 (d, J = 27.4 Hz, 1H), 3.90−3.85 (m, 1H), 3.61−3.53 (m, 1H), 3.33 (s, 3H), 2.60 (s, 3H), 2.12−2.02 (m, 1H), 1.84−1.67 (m, 1H); LC/MS (t_R = 2.45 min): m/z 308 (M + H)$^+$; chiral HPLC (wavelength 313 nm): t_R = 7.41 min, de = 98%.

2-Chloro-4-((3*S*,3a*R*,4*R*)-4-fluoro-3-methoxy-3a,4,5,6-tetrahydro-3H-pyrrolo[1,2-*b*]pyrazol-2-yl)-3-methylbenzonitrile (33). The title compound was prepared according to the procedure for **32**, using **26** as starting material, to give 12 mg (40%) of product, mp 79 °C. ^{1}H NMR (400 MHz, $CDCl_3$): δ 7.54−7.49 (m, 2H), 5.30 (s, 1H), 5.25 (d, J = 52.8 Hz, 1H), 3.84 (d, J = 29.4 Hz, 1H), 3.80−3.66 (m, 2H), 3.28 (s, 3H), 2.59 (s, 3H), 2.35−2.10 (m, 2H); LC/MS (t_R = 2.40 min): m/z 308 (M + H)$^+$; chiral HPLC (wavelength 321 nm): t_R = 6.98 min, de = 99%.

4-((3*S*,3a*S*,5*R*)-5-Hydroxy-3-methoxy-3a,4,5,6-tetrahydro-3H-pyrrolo[1,2-*b*]pyrazol-2-yl)-2-chloro-3-methylbenzonitrile (35). Methylation was carried out according to the procedure for **22**, using intermediate **20** as starting material, to afford 80 mg (77%) of **34**. Desilylation was performed according to the procedure for **26** to give 40 mg (69%) of the title compound, mp 107 °C. ^{1}H NMR (400 MHz, DMSO-d_6): δ 7.86 (d, J = 8.3 Hz, 1H), 7.65 (d, J = 8.3 Hz, 1H), 5.05 (d, J = 14.2 Hz,1H), 5.03 (d, J = 3.6 Hz, 1H), 4.30−4.20 (m, 1H), 4.03−3.99 (m,1H), 3.67−3.63 (m, 1H), 3.29−3.22 (m, 1H), 3.19 (s, 3H), 2.54 (s, 3H), 1.81−1.77 (m, 1H), 1.59−1.55 (m, 1H); IR (KBr): 3408, 2947, 2831, 2229, 1587, 1527 cm^{-1}; LC/MS (t_R = 2.08 min): m/z 306 (M + H)$^+$; chiral HPLC (wavelength 328 nm): t_R = 7.28 min, de = 99%.

2-Chloro-4-((3S,3aS,5S)-5-hydroxy-3-methoxy-3a,4,5,6-tetrahydro-3H-pyrrolo[1,2-*b*]pyrazol-2-yl)-3-methylbenzonitrile (36). The title compound was prepared according to the procedure for **30**, using **35** as starting material, to give 8 mg (28%) of product, mp 109 °C. ^{1}H NMR (400 MHz, DMSO-d_6): δ 7.85 (d, J = 8.3 Hz, 1H), 7.62 (d, J = 8.3 Hz, 1H), 5.12 (s, 1H), 4.69 (d, J = 2.5 Hz, 1H), 4.25 (s, 1H), 3.86 (t, J = 8.3 Hz, 1H), 3.43 (d, J = 12.7 Hz, 1H), 3.22 (s, 3H), 2.58 (s, 3H), 2.31 (d, J = 12.7 Hz, 1H), 1.23 (s, 1H), IR (KBr): 3527, 2941, 2872, 2235, 1589 cm^{-1}; LC/MS (t_R = 2.03 min): m/z 306 (M + H)$^+$; chiral HPLC (wavelength 320 nm): t_R = 6.73 min, de = 98%.

2-Chloro-4-((3*S*,3a*S*,5*S*)-5-fluoro-3-methoxy-3a,4,5,6-tetrahydro-3H-pyrrolo[1,2-*b*]pyrazol-2-yl)-3-methylbenzonitrile (37). The title compound was prepared according to the procedure for **32**, using **35** as starting material, to give 10 mg (20%) of product, mp 98 °C. ^{1}H NMR (400 MHz, DMSO-d_6): δ 7.87 (d, J = 8.3 Hz, 1H), 7.66 (d, J = 8.3 Hz, 1H), 5.26−5.24 (m, 1H), 5.19−5.15 (m, 1H), 3.97−3.89 (m, 2H), 3.29 (s, 3H), 2.67−2.66 (m, 1H), 2.52 (s, 3H), 1.89−1.84 (m, 2H); LC/MS (t_R = 2.32 min): m/z 308 $(M + H)^+$; chiral HPLC (wavelength 310 nm): t_R = 7.61 min, de = 98%.

2-Chloro-4-((3*S*,3a*S*)-3-methoxy-5-oxo-3a,4,5,6-tetrahydro-3H-pyrrolo[1,2-*b*]pyrazol-2-yl)-3-methylbenzonitrile (38). To a solution of **35** (18 mg, 0.059 mmol) in DCM (2 mL) at room temperature was added Dess−Martin periodinane (50 mg, 0.118 mmol), and the reaction mixture was stirred at room temperature for 24 h. Once the starting material had disappeared (monitored by TLC), the reaction mixture was diluted with DCM and washed with water, brine, dried over Na_2SO_4, and concentrated. Purification by preparative TLC (2% methanol in DCM) provided 13 mg (86%) of the title compound, mp 157 °C. ^{1}H NMR (400 MHz, DMSO-d_6): δ 7.90 (d, J = 7.9 Hz, 1H), 7.75 (d, J = 8.3 Hz, 1H), 5.16 (s, 1H), 4.43 (t, J = 9.7 Hz, 1H), 3.92 (d, J = 19.1 Hz, 1H), 3.81 (d, J = 18.6 Hz, 1H), 3.29 (s, 3H), 2.57 (s, 3H), 2.37−2.32 (m, 2H); IR (KBr): 2947, 2831, 2229, 1587 cm^{-1}; LC/MS (t_R = 2.28 min): m/z 304 $(M + H)^+$; chiral HPLC (wavelength 318 nm): t_R = 10.58 min, de = 97%.

2-Chloro-4-((3*S*,3a*S*)-5,5-difluoro-3-methoxy-3a,4,5,6-tetrahydro-3H-pyrrolo[1,2-*b*]pyrazol-2-yl)-3-methylbenzonitrile (39). To a stirred solution of **38** (30 mg, 0.0988 mmol) in DCM (3 mL) at 0 °C was added DAST (0.032 mL, 0.247 mmol) and stirred for 16 h. Once the starting material had disappeared (monitored by TLC), the reaction mixture was diluted with DCM. The organic layer was washed with water, brine, dried over Na_2SO_4, and concentrated to get crude product which was purified by preparative TLC (40% ethyl acetate in petroleum ether) to afford 10 mg (32%) of the title compound, mp 108 °C. ^{1}H NMR (400 MHz, DMSO-d_6): δ 7.91 (d, J = 8.3 Hz, 1H), 7.71 (d, J = 8.3 Hz, 1H), 5.16 (s, 1H), 4.29 (t, J = 8.8 Hz, 1H), 3.95 (t, J = 8.8 Hz, 1H), 3.77−3.70 (m, 1H), 3.25 (s, 3H), 2.66−2.60 (m, 1H), 2.50 (s, 3H), 1.18−1.10 (m, 1H); IR (KBr): 3439, 2941, 2231, 1589, 1529 cm^{-1}; LC/MS (t_R = 2.49 min): m/z 326 $(M + H)^+$; chiral HPLC (wavelength 308 nm): t_R = 6.29 min, de = 99%.

Biology. *C2C12 Reporter Gene Assay.* C2C12 cells were obtained from ATCC (LGC Standards) and maintained in DMEM (Life Technologies) modified to contain 4 mM L-glutamine, 4.5 g/L glucose, 1 mM sodium pyruvate, 1.5 g/L sodium bicarbonate and 10% heat-inactivated fetal bovine serum (FBS; PAA). Cells were seeded at 8000 cells/well in clear flat bottom 96-well plates (BD) in DMEM without phenol red (Life Technologies) containing 10% charcoal-stripped FBS (cs-FBS; Invitrogen). On the following day, cells were transfected with a 1:1 ratio (200 ng/well) of human AR expression plasmid and pGL4.26-based luciferase reporter plasmid (Promega) containing two copies of the specific androgen-response-element IDR17[40] upstream of the minimal promoter using Lipofectamine 2000 (Invitrogen). Five hours after transfection, DMSO compound stock solutions were diluted in DMEM without phenol red containing 10% cs-FBS and added to the wells maintaining a maximal final DMSO concentration of 0.5%. The next day, luciferase activities were determined using Steady-Glo Luciferase assay system (Promega) and a VICTOR plate reader (PerkinElmer). Data fitting and calculation of EC_{50} values were done using nonlinear least-squares regression in Graphpad Prism 4.0 (Graphpad Software).

Binding Assays. Binding to human AR was determined using a whole cell radioligand competition binding assay. Human breast adenocarcinoma (MDA-MB-453) cells expressing high levels of AR were cultured in DMEM containing 10% FBS. For measuring AR binding, cells were first cultured in DMEM without phenol red containing 10% cs-FBS for 24 h. Then, cells were harvested, and 300 000 cells were transferred to Eppendorf tubes in 300 μL of culture medium. Subsequently, they were incubated with 0.25 nM ^{3}H-DHT (American Radiolabeled Chemicals Inc.) and serial dilutions of test compound (maximal 0.5% DMSO) for 90 min at room temperature with gentle agitation. Cells were washed with ice-cold DMEM and then twice with PBS using centrifugations with 3000 rpm at 4 °C for 5 min. Finally, cells were lysed in 200 μL of buffer containing 2% SDS, 10% glycerol and 10 mM Tris-HCl (pH 6.8) by incubation for 30 min and intermittent vortexing every 5 min. Lysates were transferred into new tubes, and radioactivity was counted a Wallac Microbeta Trilux β counter (PerkinElmer). Binding to glucocorticoid, progesterone, and estrogen receptor α was determined applying corresponding PolarScreen assays (Life Technologies) using 50 μL of assay volumes and 4 h incubation times. Data analysis and determination of IC_{50} values were done using sigmoidal curve fitting with Graphpad Prism 4.0 (Graphpad Software).

Pharmacokinetics. All procedures with animals performed in this study were conducted according to Animal Welfare Law and specifically under the Animal License No. 812/04/A/CPCSEA. Animals were provided ad libitum with water and Tekla rodent irradiated, pelleted diet T.2014S.15 containing 14% protein (Harlan Lab). Male HanRCC:Wistar rats were obtained from in house breeding. Groups of four rats were cannulated and 2 days later injected iv with 1 mg/kg compound formulated in 10% ethanol, 2% *N*,*N*-dimethylacetamide, 50% PEG-200, and 38% normal sterile saline using a dosing volume of 2 mL/kg. Compound levels were analyzed and quantified in plasma after 0.08, 0.25, 0.5, 1, 2, 4, 6, 9, 24, and 48 h using LC-MS/MS. For sc pharmacokinetics analysis, compounds were administered at 0.5 mg/kg in PEG-200:water (50:50) using 2 mL/kg dosing volume and 0.25, 0.5, 1, 2, 4, 6, 9, 24, 32, 48, and 56 h time points. Pharmacokinetic parameters were determined using the WinNonlin software.

In Vivo Pharmacology (Hershberger Assay).[38] Briefly, rats aged 42−56 days were orchidectomized. Fourteen days later, groups of six animals were treated once daily sc for 14 days with different doses of compound in 50% PEG 200 and 50% of saline or with vehicle control at 2 mL/kg volume. In addition, a group of animals with sham surgery was equally treated with vehicle. Body weight and food consumption were recorded daily during the treatment period. On day 15 after overnight fasting, animals were weighed and blood was taken under isoflurane anesthesia 3 h after the last dosing for hematology. Separately, serum was prepared for serological analyses, and plasma samples were collected for drug concentration analysis. Subsequently, animals were euthanized by exsanguinization. Finally, ventral prostates and levator ani plus bulbo cavernosus muscles were dissected, and their wet weights were determined.

In Vitro Human Skin Permeation. Franz's diffusion cell assay[36] was used to evaluate in vitro permeation flux through human skin (abdominal cadaver dermatomed human skin ∼0.5

mm). PBS pH 7.4 (Sigma Dulbecco's PBS) was used as receptor phase after being degassed under vacuum for 2 h. At predetermined time points, 300 μL of receptor solution was collected and replaced by fresh media. In vitro human skin permeation was conducted at 32 °C. Three different human donors were used for the assessment of the intrinsic permeation of compounds through the skin. Infinite dose studies (concentration in the receptor phase remained constant throughout the study) were conducted by providing a saturated suspension formulation of the compounds in a vehicle composed of 0.5% Brij 98 in PBS pH 7.4. Brij 98, a nonionic surfactant, was used to provide an excess of drug in solution and to prevent the permeation to be limited by dissolution, in particular, for insoluble compounds. It has been shown that the use of aqueous solutions containing 6% Brij 98 has a negligible effect on the flux of compounds across the skin.[41] Occlusion was achieved by closing the receptor compartment with Parafilm. Scientist Version 3.0 (Micromath Inc., Salt Lake City, UT, United States) was used to fit diffusion equations to experimental data and to estimate steady-state flux values.

Crystallography and Structure Determination of the AR Complex with 26. The ligand binding domain of human AR (AR-LBD; residues 663−919) was expressed in *Escherichia coli* BL21DE3 cells as a GST fusion protein. The cells were grown to an OD of 0.6 and induced with 0.1 mM IPTG at 15 °C for 20 h. Protein was expressed in the presence of 50 μM **26**. Protein was purified using a glutathione-Sepharose column followed by cleavage of the GST tag. Further purification was performed using sequentially the amino-benzimidine, Hi-Trap SP Sepharose, and S-75 columns. Crystallization of AR-LBD with **26** was setup by hanging drop vapor diffusion technique with 7 mg/mL protein. Crystals appeared in 2 days at room temperature. The cocrystals were flash-frozen at 100 K using 20% glycerol as cryo-protectant. The diffraction data sets were collected using in-house Rigaku RU300 X-ray generator with R-AXIS IV++ detector to a maximum resolution of 2.1 Å. Data indexing, integration, and scaling were performed using DENZO and SCALEBPCK.[42] The structure was solved by molecular replacement (MR) method using the PDB submission 1Z95 as the search model. Alternate cycles of restrained refinement and manual rebuilding were performed with the programs REFMAC 5.2.0001[43,44] and Coot,[45] respectively. A portion (5%) of the reflections were randomly excluded from the refinement to monitor the free residual-factor (R_{free}). A summary of the data reduction and structure refinement statistics is provided in Table 5. Coordinates of the X-ray structure have been deposited in the Protein Data Bank (accession code 4QL8).

Molecular Docking. The cocrystal structure of **26** in complex with AR-LBD was employed for setting up molecular docking protocols. Prior to this, the protein coordinates were optimized through suitable bond-order assignments, water molecules elimination (except the one bridging with Arg752 and Met745), addition of hydrogen atoms, internal hydrogen bonds refinement, and restrained minimization through OPLS 2005 force-field. Hydrogen bonding constraints were applied to Asn705, Arg752 and Thr807 side-chains during receptor grid generation so that they can be used in docking (if required). The molecules were energy-minimized through LigPrep and then docked into generated grid (AR-LBD active-site) employing standard precision modes using Glide software. All software names mentioned in this section are products of Schrödinger Inc., and all images were prepared using PyMOL (also a product of Schrödinger Inc.).

Table 5. Diffraction Data and Refinement Statistics for 26

space group	$P2_12_12_1$
cell parameters (Å)	a = 55.129, b = 65.476, c = 68.964
diffraction resolution (Å)	50.0−2.10
total reflections	42 722
unique reflections	14 439
completeness (%)	96.8 (80.4)[a]
R_{sym}	0.048(0.134)
$I/\sigma I$	19.3 (3.2)
multiplicity	3.5(3.3)
refinement	
resolution (Å)	29.62−2.1
no. of reflections	13 660
completeness (%)	94.73(89.28)
R_{work}/R_{free}	0.245/0.275
mean B-factors	20.403
rms bond (Å)	0.005
rms angles (deg)	0.784

[a]Values corresponding to the outermost shell are given within parentheses.

■ ASSOCIATED CONTENT

Accession Codes

PDB Code: **26**, 4QL8

■ AUTHOR INFORMATION

Corresponding Authors

*E-mail: thomas.ullrich@novartis.com. Tel.: +41 61-696-3137.
*E-mail: hansjoerg.keller@novartis.com. Tel.: +41 61-696-8628.

Present Address

¶Bharat Lagu: Mitokyne, 1030 Massachusetts Avenue, Cambridge, MA 02138, United States.

Notes

The authors declare no competing financial interest.

■ ACKNOWLEDGMENTS

We thank Céline Le Bourdonnec, Pierre-Alain Carrupt and Sophie Martel from the University of Geneva, Switzerland, for conducting and interpreting the skin PAMPA experiments, Naveen Kumar R. for his help with performing in vivo pharmacological studies, and Karthikeyan N. A. for supporting the molecular modeling activities. We also gratefully acknowledge Karin Briner and Brian Richardson for their scientific and strategic support and Lawrence G. Hamann for the thorough review of the manuscript.

■ ABBREVIATIONS USED

AR, androgen receptor; BAV, bioavailability; BLA, bulbocavernosus/levator ani muscle; DAST, diethylaminosulfur trifluoride; DHT, 5α-dihydrotestosterone; ER, estrogen receptor; GR, glucocorticoid receptor; ORX, orchidectomized; PAMPA, parallel artificial membrane permeability assay; PR, progesterone receptor; SARM, selective androgen receptor modulator; Sol, aqueous solubility; T, testosterone; TBAF, tetrabutylammonium fluoride; TP, testosterone propionate

REFERENCES

(1) Palvimo, J. J. The androgen receptor. *Mol. Cell. Endocrinol.* **2012**, *352*, 1−3.

(2) Matsumoto, T.; Sakari, M.; Okada, M.; Yokoyama, A.; Takahashi, S.; Kouzmenko, A.; Kato, S. The androgen receptor in health and disease. *Annu. Rev. Physiol.* **2013**, *75*, 20.1−20.24.

(3) Bhasin, S.; Woodhouse, L.; Casaburi, R.; Singh, A. B.; Mac, R. P.; Lee, M.; Yarasheski, K. E.; Sinha-Hikim, I.; Dzekov, C.; Dzekov, J.; Magliano, L.; Storer, T. W. Older men are as responsive as young men to the anabolic effects of graded doses of testosterone on the skeletal muscle. *J. Clin. Endocrinol. Metab.* **2005**, *90*, 678−688.

(4) Horstman, A. M.; Dillon, E. L.; Urban, R. J.; Sheffield-Moore, M. The role of androgens and estrogens on healthy aging and longevity. *J. Gerontol., Ser. A* **2012**, *67*, 1140−1152.

(5) O'Connell, M. D.; Wu, F. C. Androgen effects on skeletal muscle: implications for the development and management of frailty. *Asian J. Androl.* **2014**, *16*, 203−212.

(6) Kallman, D. A.; Plato, C. C.; Tobin, J. D. The role of muscle loss in the age-related decline of grip strength: cross-sectional and longitudinal perspectives. *J. Gerontol.* **1990**, *45*, M82−M88.

(7) Wu, F. C.; Tajar, A.; Pye, S. R.; Silman, A. J.; Finn, J. D.; O'Neill, T. W.; Bartfai, G.; Casanueva, F.; Forti, G.; Giwercman, A.; Huhtaniemi, I. T.; Kula, K.; Punab, M.; Boonen, S.; Vanderschueren, D. Hypothalamic−pituitary−testicular axis disruptions in older men are differentially linked to age and modifiable risk factors: the European Male Aging Study. *J. Clin. Endocrinol. Metab.* **2008**, *93*, 2737−2745.

(8) Hyde, Z.; Flicker, L.; Almeida, O. P.; Hankey, G. J.; McCaul, K. A.; Chubb, S. A.; Yeap, B. B. Low free testosterone predicts frailty in older men: the health in men study. *J. Clin. Endocrinol. Metab.* **2010**, *95*, 3165−3172.

(9) Morley, J. E.; Malmstrom, T. K. Frailty, sarcopenia, and hormones. *Endocrinol. Metab. Clin. North Am.* **2013**, *42*, 391−405.

(10) Corona, G.; Rastrelli, G.; Vignozzi, L.; Maggi, M. Emerging medication for the treatment of male hypogonadism. *Expert Opin. Emerg. Drugs* **2012**, *17*, 239−259.

(11) Giannoulis, M. G.; Martin, F. C.; Nair, K. S.; Umpleby, A. M.; Sonksen, P. Hormone replacement therapy and physical function in healthy older men. Time to talk hormones? *Endocr. Rev.* **2012**, *33*, 314−377.

(12) Huhtaniemi, I. Late onset hypogonadism: current concepts and controversies of pathogenesis, diagnosis and treatment. *Asian J. Androl.* **2014**, *16*, 192−202.

(13) McEwan, I. J. Androgen receptor modulators: a marriage of chemistry and biology. *Future Med. Chem.* **2013**, *5*, 1109−1120.

(14) Zhang, X.; Sui, Z. Deciphering the selective androgen receptor modulators paradigm. *Expert Opin. Drug Discovery* **2013**, *8*, 191−218.

(15) Dalton, J. T.; Barnette, K. G.; Bohl, C. E.; Hancock, M. L.; Rodriguez, D.; Dodson, S. T.; Steiner, M. S. The selective androgen receptor modulator GTx-024 (enobosarm) improves lean body mass and physical function in healthy elderly men and postmenopausal women: Results of a double-blind, placebo-controlled phase II trial. *J. Cachexia Sarcopenia Muscle* **2011**, *2*, 153−161.

(16) Dobs, A. S.; Boccia, R. V.; Croot, C. C.; Gabrail, N. Y.; Dalton, J. T.; Hancock, M. L.; Johnston, M. A.; Steiner, M. S. Effects of enobosarm on muscle wasting and physical function in patients with cancer: a double-blind, randomised controlled phase 2 trial. *Lancet Oncol.* **2013**, *14*, 335−345.

(17) Basaria, S.; Collins, L.; Dillon, E. L.; Orwoll, K.; Storer, T. W.; Miciek, R.; Ulloor, J.; Zhang, A.; Eder, R.; Zientek, H.; Gordon, G.; Kazmi, S.; Sheffield-Moore, M.; Bhasin, S. The safety, pharmacokinetics, and effects of LGD-4033, a novel nonsteroidal oral, selective androgen receptor modulator, in healthy young men. *J. Gerontol., Ser. A* **2013**, *68*, 87−95.

(18) Papanicolaou, D. A.; Ather, S. N.; Zhu, H.; Zhou, Y.; Lutkiewicz, J.; Scott, B. B.; Chandler, J. A phase IIA randomized, placebo-controlled clinical trial to study the efficacy and safety of the selective androgen receptor modulator (SARM), MK-0773 in female participants with sarcopenia. *J. Nutr. Health Aging* **2013**, *17*, 533−543.

(19) Westaby, D.; Ogle, S. J.; Paradinas, F. J.; Randell, J. B.; Murray-Lyon, I. M. Liver damage from long-term methyltestosterone. *Lancet* **1977**, *2*, 262−263.

(20) Hameed, A.; Brothwood, T.; Bouloux, P. Delivery of testosterone replacement therapy. *Curr. Opin. Investig. Drugs* **2003**, *4*, 1213−1219.

(21) Thevis, M.; Schanzer, W. Synthetic anabolic agents: steroids and nonsteroidal selective androgen receptor modulators. *Handb. Exp. Pharmacol.* **2010**, 99−126.

(22) Wang, C.; Swerdloff, R. S.; Iranmanesh, A.; Dobs, A.; Snyder, P. J.; Cunningham, G.; Matsumoto, A. M.; Weber, T.; Berman, N. Transdermal testosterone gel improves sexual function, mood, muscle strength, and body composition parameters in hypogonadal men. *J. Clin. Endocrinol. Metab.* **2000**, *85*, 2839−2853.

(23) Choy, Y. B.; Prausnitz, M. R. The rule of five for non-oral routes of drug delivery: ophthalmic, inhalation and transdermal. *Pharm. Res.* **2011**, *28*, 943−948.

(24) Lambers, H.; Piessens, S.; Bloem, A.; Pronk, H.; Finkel, P. Natural skin surface pH is on average below 5, which is beneficial for its resident flora. *Int. J. Cosmet. Sci.* **2006**, *28*, 359−370.

(25) Margetts, L.; Sawyer, R. Transdermal drug delivery: principles and opioid therapy. *Contin. Educ. Anaesth. Crit. Care Pain* **2007**, *7*, 171−176.

(26) Ostrowski, J.; Kuhns, J. E.; Lupisella, J. A.; Manfredi, M. C.; Beehler, B. C.; Krystek, S. R., Jr.; Bi, Y.; Sun, C.; Seethala, R.; Golla, R.; Sleph, P. G.; Fura, A.; An, Y.; Kish, K. F.; Sack, J. S.; Mookhtiar, K. A.; Grover, G. J.; Hamann, L. G. Pharmacological and X-ray structural characterization of a novel selective androgen receptor modulator: Potent hyperanabolic stimulation of skeletal muscle with hypostimulation of prostate in rats. *Endocrinology* **2007**, *148*, 4−12.

(27) Li, J. J.; Sutton, J. C.; Nirschl, A.; Zou, Y.; Wang, H.; Sun, C.; Pi, Z.; Johnson, R.; Krystek, S. R., Jr.; Seethala, R.; Golla, R.; Sleph, P. G.; Beehler, B. C.; Grover, G. J.; Fura, A.; Vyas, V. P.; Li, C. Y.; Gougoutas, J. Z.; Galella, M. A.; Zahler, R.; Ostrowski, J.; Hamann, L. G. Discovery of potent and muscle selective androgen receptor modulators through scaffold modifications. *J. Med. Chem.* **2007**, *50*, 3015−3025.

(28) Lemke, T. L.; Williams, D. A.; Roche, V. F.; Zito, S. W. *Foye's Principles of Medicinal Chemistry*, 7th ed.; Wolters Kluwer/Lippincott Williams & Wilkins: Philadelphia, 2013; p 549.

(29) Manfredi, M. C.; Bi, Y.; Nirschl, A. A.; Sutton, J. C.; Seethala, R.; Golla, R.; Beehler, B. C.; Sleph, P. G.; Grover, G. J.; Ostrowski, J.; Hamann, L. G. Synthesis and SAR of tetrahydropyrrolo[1,2-b][1,2,5]-thiadiazol-2(3H)-one 1,1-dioxide analogues as highly potent selective androgen receptor modulators. *Bioorg. Med. Chem. Lett.* **2007**, *17*, 4487−4490.

(30) Shen, J.-K.; Katayama, H. Preparation of pyrazole and pyrazoline derivatives by intramolecular reaction of hydrazones. *Chem. Lett.* **1992**, *3*, 451−452.

(31) Sun, C.; Robl, J. A.; Wang, T. C.; Huang, Y.; Kuhns, J. E.; Lupisella, J. A.; Beehler, B. C.; Golla, R.; Sleph, P. G.; Seethala, R.; Fura, A.; Krystek, S. R., Jr.; An, Y.; Malley, M. F.; Sack, J. S.; Salvati, M. E.; Grover, G. J.; Ostrowski, J.; Hamann, L. G. Discovery of potent, orally-active, and muscle-selective androgen receptor modulators based on an N-aryl-hydroxybicyclohydantoin scaffold. *J. Med. Chem.* **2006**, *49*, 7596−7599.

(32) Potts, R. O.; Guy, R. H. Predicting skin permeability. *Pharm. Res.* **1992**, *9*, 663−669.

(33) Ottaviani, G.; Martel, S.; Carrupt, P. A. Parallel artificial membrane permeability assay: a new membrane for the fast prediction of passive human skin permeability. *J. Med. Chem.* **2006**, *49*, 3948−3954.

(34) Ottaviani, G.; Martel, S.; Carrupt, P. A. In silico and in vitro filters for the fast estimation of skin permeation and distribution of new chemical entities. *J. Med. Chem.* **2007**, *50*, 742−748.

(35) Bartosova, L.; Bajgar, J. Transdermal drug delivery in vitro using diffusion cells. *Curr. Med. Chem.* **2012**, *19*, 4671−4677.

(36) Organisation for Economic Co-operation and Development (OECD). OECD guideline for the testing of chemicals. Skin absorption: in vitro method; OECD: Paris, 2004; Vol. *428*, 1−8

(37) Nicolazzo, J. A.; Morgan, T. M.; Reed, B. L.; Finnin, B. C. Synergistic enhancement of testosterone transdermal delivery. *J. Controlled Release* **2005**, *103*, 577−585.

(38) Hershberger, L. G.; Shipley, E. G.; Meyer, R. K. Myotrophic activity of 19-nortestosterone and other steroids determined by modified levator ani muscle method. *Proc. Soc. Exp. Biol. Med.* **1953**, *83*, 175−180.

(39) Aldridge, W. S., III; Hornstein, B. J.; Serron, S.; Dattelbaum, D. M.; Schoonover, J. R.; Meyer, T. J. Synthesis and characterization of oligoproline-based molecular assemblies for light harvesting. *J. Org. Chem.* **2006**, *71*, 5186−5190.

(40) Zhou, Z.; Corden, J. L.; Brown, T. R. Identification and characterization of a novel androgen response element composed of a direct repeat. *J. Biol. Chem.* **1997**, *272*, 8227−8235.

(41) Bronaugh, R. L. Methods for in vitro percutaneous absorption. *Toxicol. Mech. Methods* **1995**, *5*, 265−273.

(42) Otwinowski, Z.; Minor, W. Processing of X-ray diffraction data collected in oscillation mode. In *Methods in Enzymology*; Carter, C. W., Sweet, R. M., Eds.; Academic Press, Inc.: New York, 1997; pp 307−326.

(43) Collaborative Computational Project, N. 4. The CCP4 suite: programs for protein crystallography. *Acta Crystallogr. D. Biol. Crystallogr.* **1994**, *50*, 760−763.

(44) Murshudov, G. N.; Vagin, A. A.; Dodson, E. J. Refinement of macromolecular structures by the maximum-likelihood method. *Acta Crystallogr. D. Biol. Crystallogr.* **1997**, *53*, 240−255.

(45) Emsley, P.; Cowtan, K. Coot: model-building tools for molecular graphics. *Acta Crystallogr. D. Biol. Crystallogr.* **2004**, *60*, 2126−213.